AD-A122 165 STRUCTURAL EVALUATION OF AN ADVANCED COMPOSITE HYDROFOIL FOIL-COMPONENT(U) DAVID W TAYLOR NAVAL SHIP RESEARCH AND DEVELOPMENT CENTER BETHESDA MD 1/1

UNCLASSIFIED W P COUCH ET AL. NOV 82 DTNSRDC-82/082 F/G 14/2 NL

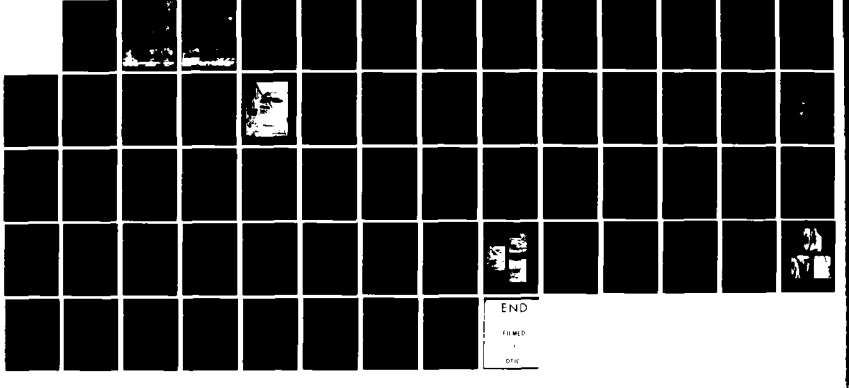

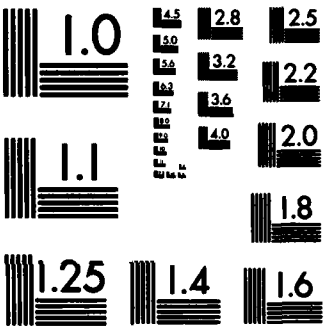

DTNSRDC-82/082

DAVID W. TAYLOR NAVAL SHIP RESEARCH AND DEVELOPMENT CENTER

Bethesda, Maryland 20084

STRUCTURAL EVALUATION OF AN ADVANCED COMPOSITE HYDROFOIL FOIL COMPONENT

William P. [illegible]
Longin Stankiewicz
Henry Chaskalis

APPROVED FOR PUBLIC RELEASE: DISTRIBUTION UNLIMITED

STRUCTURAL EVALUATION OF AN ADVANCED COMPOSITE HYDROFOIL FOIL COMPONENT

MAJOR DTNSRDC ORGANIZATIONAL COMPONENTS

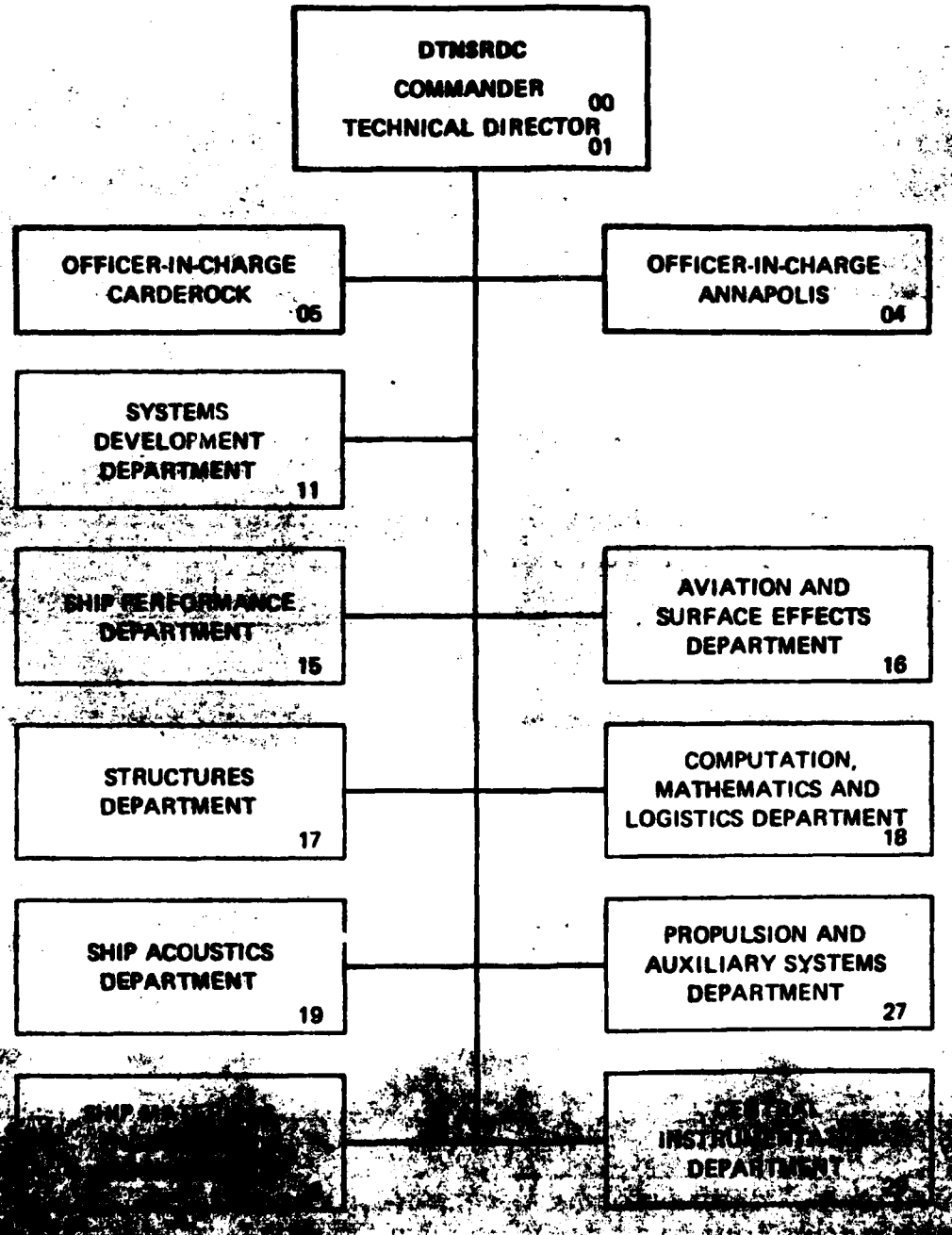

UNCLASSIFIED

SECURITY CLASSIFICATION OF THIS PAGE (When Data Entered)

REPORT DOCUMENTATION PAGE		READ INSTRUCTIONS BEFORE COMPLETING FORM
1. REPORT NUMBER DTNSRDC-82/082	2. GOVT ACCESSION NO. AD-A122165	3. RECIPIENT'S CATALOG NUMBER
4. TITLE (and Subtitle) Structural Evaluation of an Advanced Composite Hydrofoil Foil Component		5. TYPE OF REPORT & PERIOD COVERED Final 6. PERFORMING ORG. REPORT NUMBER
7. AUTHOR(s) William P. Couch, Longin Greszczuk and Henry Chaskelis		8. CONTRACT OR GRANT NUMBER(s)
9. PERFORMING ORGANIZATION NAME AND ADDRESS David W. Taylor Naval Ship Research and Development Center Bethesda, Md. 20084		10. PROGRAM ELEMENT, PROJECT, TASK AREA & WORK UNIT NUMBERS Program Element 62543N Project SF43400391 Work Unit 1730-035
11. CONTROLLING OFFICE NAME AND ADDRESS Naval Sea Systems Command Code 03R24 Washington, D.C. 20362		12. REPORT DATE November 1982 13. NUMBER OF PAGES 62
14. MONITORING AGENCY NAME & ADDRESS(if different from Controlling Office)		15. SECURITY CLASS. (of this report) UNCLASSIFIED 15a. DECLASSIFICATION/DOWNGRADING SCHEDULE

16. DISTRIBUTION STATEMENT (of this Report)

APPROVED FOR PUBLIC RELEASE: DISTRIBUTION UNLIMITED

17. DISTRIBUTION STATEMENT (of the abstract entered in Block 20, if different from Report)

18. SUPPLEMENTARY NOTES

19. KEY WORDS (Continue on reverse side if necessary and identify by block number)

Hydrofoils, strut-foil systems, control flaps, composite materials, graphite epoxy

20. ABSTRACT (Continue on reverse side if necessary and identify by block number)

An advanced composite foil test component (tapered box beam) was designed by the McDonnell Douglas Astronautics Company under contract to the Naval Sea Systems Command. Two identical box beams were fabricated for static and fatigue testing. Each consisted of two hybrid graphite epoxy skins bolted and bonded to three HY-130 steel spars. The box beams were tested at the David W. Taylor Naval Ship Research and Development Center to determine their structural behavior under a cantilever bending stress distribution due to a concentrated load, to establish a load versus stress relationship for the simulated sea load fatigue test, and to compare their response to cyclic loading with that of candidate metallic designs. In addition, initial flaws and

(Continued on reverse side)

DD FORM 1 JAN 73 1473 EDITION OF 1 NOV 65 IS OBSOLETE
S/N 0102-LF-014-6601

UNCLASSIFIED

SECURITY CLASSIFICATION OF THIS PAGE (When Data Entered)

(Block 20 continued)

subsequent damage as a result of static and cyclic loading were evaluated by the Naval Research Laboratory, the McDonnell Douglas Astronautics Company, and the Electric Boat Division of General Dynamics using various ultrasonic testing techniques.

Initially, Box Beam 1 incurred delaminations to the inner surface of the tensile skin in the load application area at 80 percent of the preliminary maximum operating load (foil broach) of 60 kips. Attempted repairs and modifications in this area failed to "fix" this problem, and a subsequent proof test to 60 kips resulted in extensive delaminations to both surfaces of both skins; however, there did not appear to be any significant "through-the-thickness" damage as evaluated by ultrasonic test techniques. Box Beam 1 failed after incurring 19,000 cycles of a planned 7.5×10^6 cycle spectrum fatigue test.

Box Beam 2 was initially tested to a static load of 30 kips to aid in the evaluation of out-of-plane stresses which were felt to have been the cause of failure to Box Beam 1. The results of this test were inconclusive. The box beam was then tested to a static load of 42 kips, which represented the maximum operating load excluding the broaching load. It then incurred 920,000 cycles before failure under the operational cyclic spectra excluding the broaching load.

TABLE OF CONTENTS

LIST OF FIGURES

LIST OF TABLES

ABSTRACT

An advanced composite foil test component (tapered box beam) was designed by the McDonnell Douglas Astronautics Company under contract to the Naval Sea Systems Command. Two identical box beams were fabricated for static and fatigue testing. Each consisted of two hybrid graphite epoxy skins bolted and bonded to three HY-130 steel spars. The box beams were tested at the David W. Taylor Naval Ship Research and Development Center to determine their structural behavior under a cantilever bending stress distribution due to a concentrated load, to establish a load versus stress relationship for the simulated sea load fatigue test, and to compare their response to cyclic loading with that of candidate metallic designs. In addition, initial flaws and subsequent damage as a result of static and cyclic loading were evaluated by the Naval Research Laboratory, the McDonnell Douglas Astronautics Company, and the Electric Boat Division of General Dynamics using various ultrasonic testing techniques.

Initially, Box Beam 1 incurred delaminations to the inner surface of the tensile skin in the load application area at 80 percent of the preliminary maximum operating load of 60 (foil broach) kips. Attempted repairs and modifications in this area failed to "fix" this problem, and a subsequent proof test to 60 kips resulted in extensive delaminations to both surfaces of both skins; however, there did not appear to be any significant "through-the-thickness" damage as evaluated by ultrasonic test techniques. Box Beam 1 failed after incurring 19,000 cycles of a planned 7.5×10^6 cycle spectrum fatigue test.

Box Beam 2 was initially tested to a static load of 30 kips to aid in the evaluation of out-of-plane stresses which were felt to have been the cause of failure to Box Beam 1. The results of this test were inconclusive. The box beam was then tested to a static load of 42 kips, which represented the maximum operating load excluding the broaching load. It then incurred 920,000 cycles before failure under the operational cyclic spectra excluding the broaching load.

ADMINISTRATIVE INFORMATION

This investigation is part of an Exploratory Development Program, sponsored by the Naval Sea Systems Command (NAVSEA 03R24 and 05R15). The work was performed at the David W. Taylor Naval Ship Research and Development Center under Program Element 62543N, Project SF 43 400 391, and Work Unit 1730-035. Mr. Longin Greszczuk is an employee of the McDonnell Douglas Astronautics Company, and Mr. Henry Chaskelis is an employee of the Naval Research Laboratory.

INTRODUCTION

The David W. Taylor Naval Ship Research and Development Center (DTNSRDC) has been conducting a program to evaluate the use of advanced composites for advanced naval ship structures. As a result of feasibility studies performed by the McDonnell Douglas Astronautics Company[1]* and the Grumman Aerospace Corporation[2] and a review of high payoff areas for structural application of advanced composites by the Naval Ship Composites Community,** the hydrofoil strut-foil system was selected as the primary structural element to assess the current technology status of advanced composites for marine application. Two foil test components (tapered box beams) consisting of hybrid graphite epoxy (GR EP) skins and HY-130 steel spars were designed and fabricated by McDonnell Douglas.[3] This design represents a strut-foil system having an approximate weight savings of 25 percent compared to current metallic strut-foil systems fabricated entirely of steel with a yield strength of 130 ksi. It was originally planned*** that the two box beams were to be tested in fatigue, one in air and one in salt water, to assess the fatigue behavior of a typical graphite epoxy structure under simulated sea loads and to compare that behavior with several metallic designs. Due to premature failures in the region of load application, both box beams were cyclically tested in air only. This report describes the static tests, ultrasonic nondestructive evaluations (NDE), repair procedures, and cyclic tests for the two composite box beams.

BACKGROUND: DESIGN-ANALYSIS AND FABRICATION

During the preliminary design phase, several concepts were developed and the subject design was selected for further investigation. The design rationale, laminate sizing methodology, and property prediction theories have been documented in Reference 4. The laminate skin associated with the subject design concept consists of 53 plies (~58 percent) of T-300/5208 at 0-deg orientation and 32 plies (~ 42 percent) of GY-70/5208 at $\pm$ 45-deg orientation. The 85 plies making up the 0.5 in. thick hybrid composite were dispersed according to the following layup:

---

*A complete listing of reference is given on page 55.

**NAVSEA "Long Range Research and Development Plan for Advanced Composites for High Performance Surface Ships," Review Draft (27 Sep 1974).

***Couch, W.P., "Advanced Composite Box Beam: Laboratory Evaluation and Technology Assessment Plan," DTNSRDC Technical Memorandum M-82 (Sep 1977).

$$[0°, (0_3°, \pm 45°)_8, 0_3°, (\mp 45°, 0_3°)_8, 0°]$$

During the design verification phase, the laminate was characterized to validate the theory used to predict the elastic and ultimate strength properties for a hybrid laminate; see Table 1. All averaged experimental data agreed with predicted properties within 7.4 percent. An in-depth evaluation was then conducted of the joints used in the box beam. The two basic joints were a bolted and bonded connection of the composite skins to the HY-130 steel spars, and a bonded scarf joint for connecting the composite skins to the HY-130 steel transition plates at the base of the box beam. As a result of the joint evaluation, a composite ultimate strength allowable of 68 ksi was used to develop the static and cyclic load levels. At this composite stress level, the HY-130 steel spar stress was 122 ksi; a value equal to 94 percent of the yield strength. Thus, the combination of composite and metal is such that both materials are being used at almost maximum structural efficiency.

TABLE 1 - COMPARISON OF PREDICTED AND EXPERIMENTAL MECHANICAL LAMINATE PROPERTIES

Property	Predicted	Experimental
Longitudinal Tensile Modulus, E_{L_T}	12.6×10^6 psi	13.04×10^6 psi
Transverse Tensile Modulus, E_{T_T}	4.6×10^6 psi	4.17×10^6 psi
Longitudinal Compressive Modulus, E_{L_C}	—	11.92×10^6 psi
Transverse Compressive Modulus, E_{T_C}	—	4.06×10^6 psi
Shear Modulus, G_{LT}	5.1×10^6 psi	5.09×10^6 psi
Major Tensile Poisson's Ratio, ν_{LT_T}	0.80	0.766
Minor Tensile Poisson's Ratio, ν_{TL_T}	0.29	0.244
Major Compressive Poisson's Ratio, ν_{LT_C}	—	0.634
Minor Compressive Poisson's Ratio, ν_{TL_L}	—	0.216
Longitudinal Tensile Strength, σ_{L_T}	101 ksi	105.8 ksi
Transverse Tensile Strength, σ_{T_T}	20 ksi	17.0 ksi
Longitudinal Compressive Strength, σ_{L_C}	96 ksi	94.8 ksi
Transverse Compressive Strength, σ_{T_C}	26 ksi	21.7 ksi

The final box beam design is shown schematically in Figure 1, whereas a detailed design is documented in Reference 4. Following the design of the box beam, a NASTRAN two-dimensional finite element analysis* was performed to verify the design. Figure 2 compares the bending stresses in the box beam obtained by: (1) NASTRAN finite element analysis, (2) strength-of-materials calculations, and (3) experimental strain gage results. The box beams were then fabricated and inspected by McDonnell Douglas using ultrasonics, dye penetrants, x-ray analysis, and a Fokker bond tester. From this series of nondestructive tests, it was concluded that no major delaminations, debonds, or anomalies existed in the skins or the scarf joint regions.

STATIC TESTS

BOX BEAM 1

Description of Test Procedures

The box beam was instrumented with foil-type electrical resistance strain gages as shown in Figure 3 in order to:

1. Determine the elastic behavior of the box beam structure and compare it with the strength of materials and NASTRAN stress analyses,
2. Determine the stress distribution through the thickness of the composite laminate, and
3. Monitor the box beams for changes in elastic behavior during the cyclic test.

Table 2 gives the dimensional location and function for each of the 50 gages placed on the box beam by McDonnell Douglas after the laminates were cured, but prior to assembly of the box beam. Since the gages had to be bonded to the steel spar and composite laminate prior to final assembly of the box beam, a gage type and adhesive were specified that could withstand the cure temperature of 350°F and pressure of 30 psi. The final step in the instrumentation procedure was to waterproof the gages to prevent failure due to exposure to humidity over a long period of time or to the planned saltwater test environment.

Following the manufacturer's nondestructive evaluation, the box beam was sent to the Naval Research Laboratory (NRL) for further evaluation.[5] The NRL identified three

*Stein, M.C., "A NASTRAN Analysis of a Composite Box Beam for Application to Navy Hydrofoils," DTNSRDC Technical Memorandum SD 78-173-8 (Nov 1977).

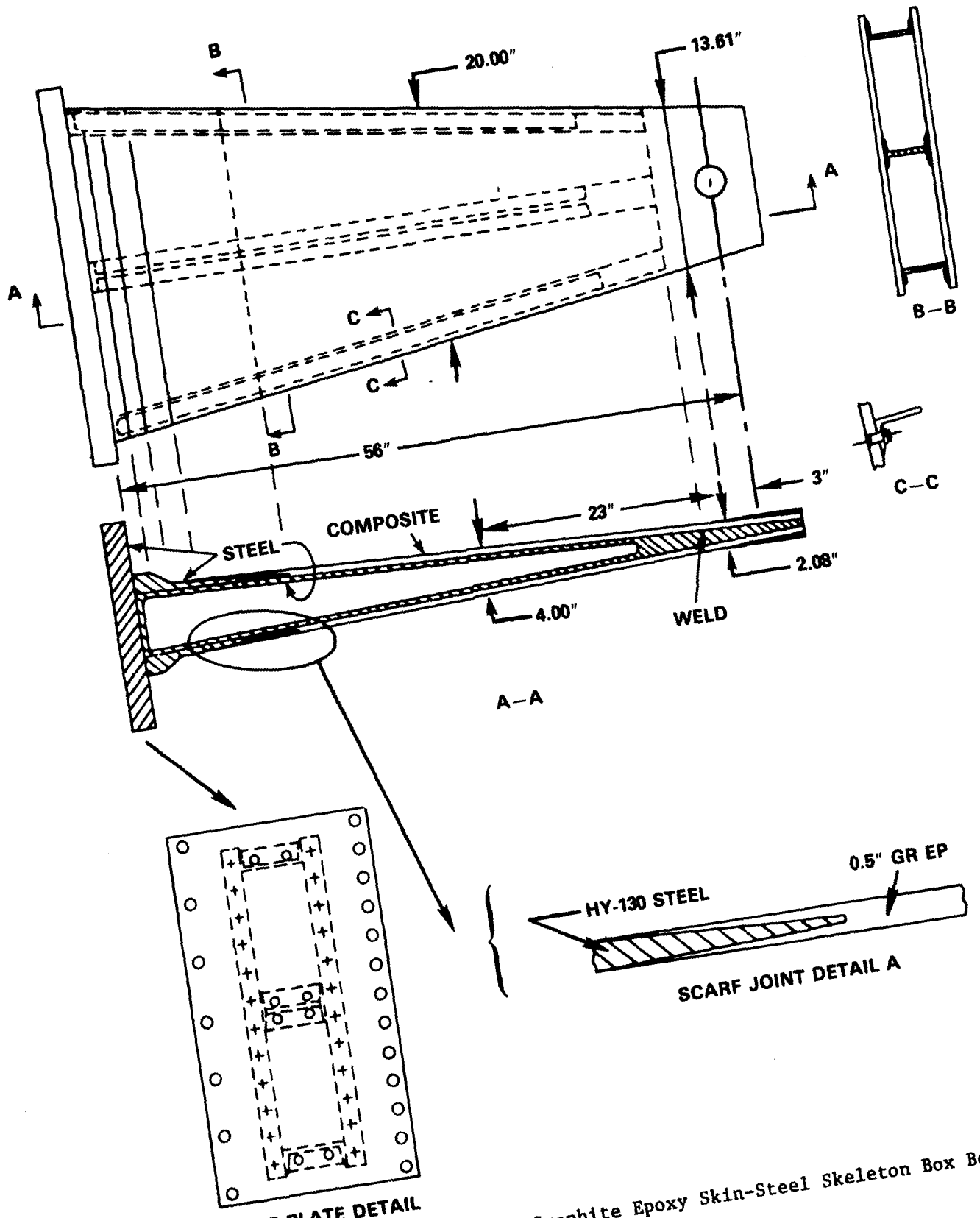

Figure 1 - Schematic of Hybrid Graphite Epoxy Skin-Steel Skeleton Box Beam

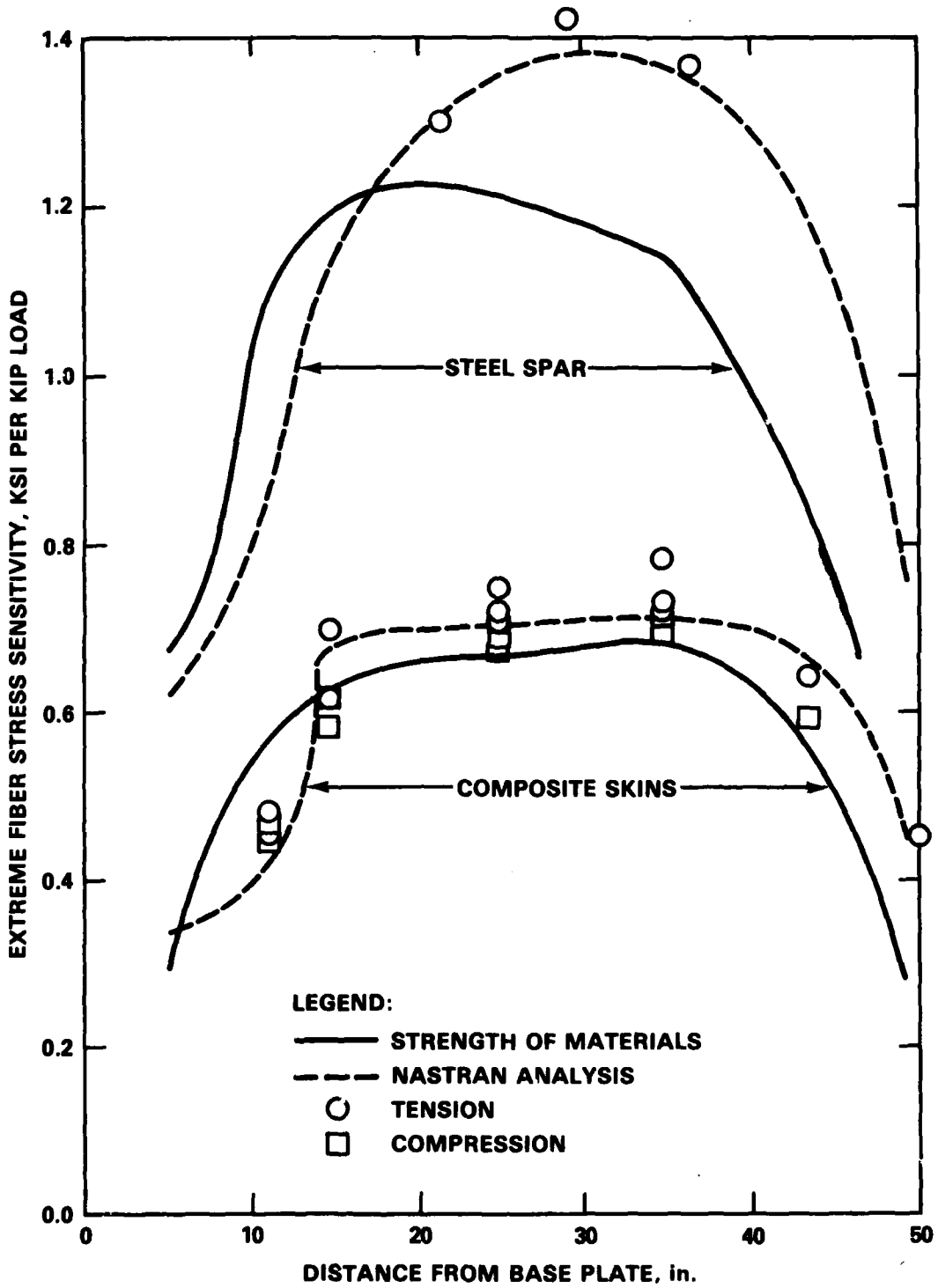

Figure 2 - Comparison of Longitudinal Bending Stresses (Extreme Fiber) in Composite Skin and Steel Spar: Experimental versus Theoretical

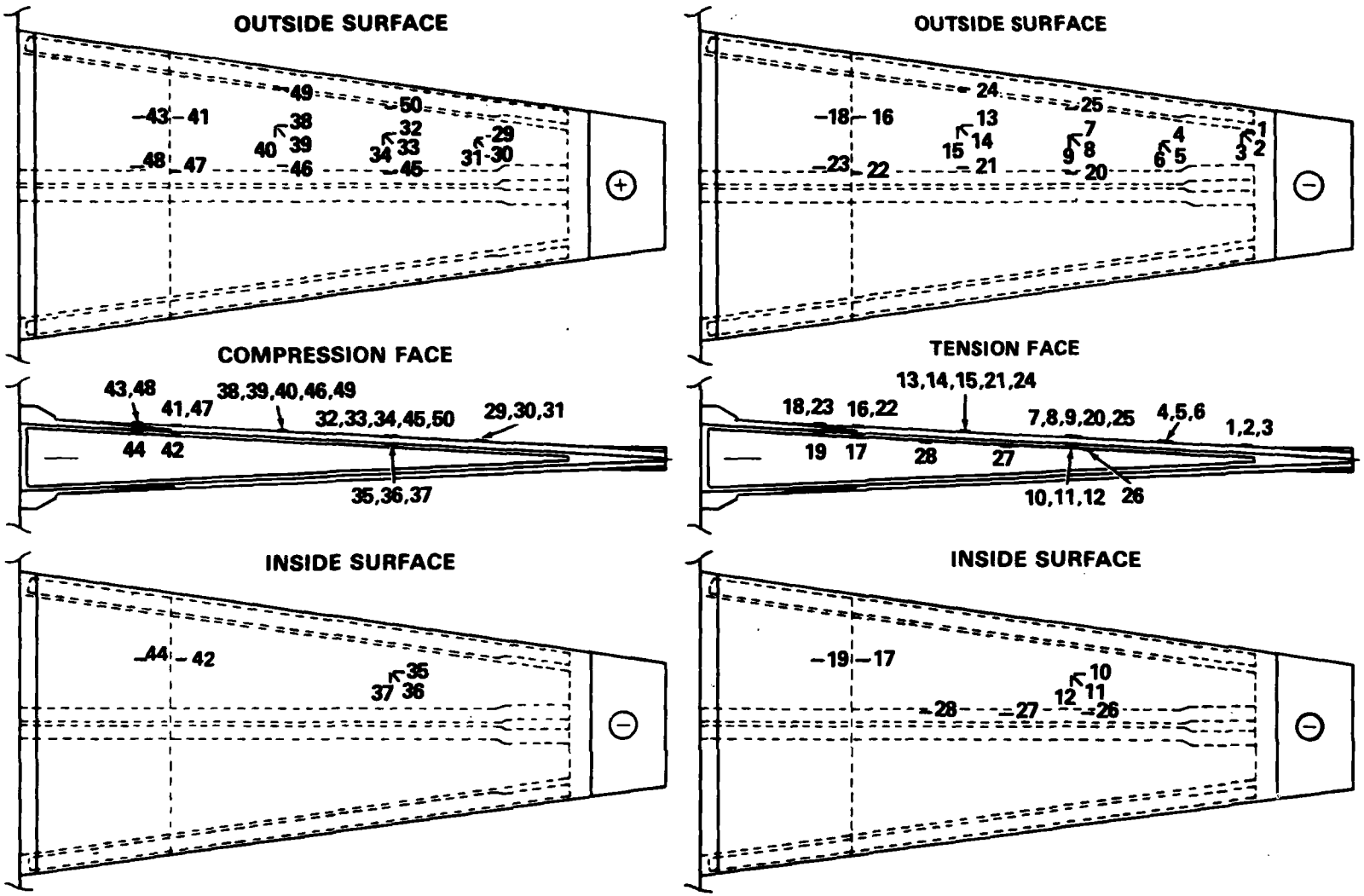

Figure 3 - Location of Strain Gages

TABLE 2 - STRAIN GAGE LOCATION AND FUNCTION

Strain Gage	Designation	Location	Coordinates x	Coordinates y	Remarks
1	Rosette Arm I-0°	Tension-Outside	50.25	+4.5	Rosette I located on section of maximum shear stress
2	Rosette Arm I-45°	Tension-Outside	50.25	+4.5	
3	Rosette Arm I-90°	Tension-Outside	50.25	+4.5	
4	Rosette Arm II-0°	Tension-Outside	43.0	3.9	For longitudinal stress distribution and in-plane shear
5	Rosette Arm II-45°	Tension-Outside	43.0	3.9	
6	Rosette Arm II-90°	Tension-Outside	43.0	3.9	
7	Rosette Arm III-0°	Tension-Outside	34.5	4.4	Rosette III located over Rosette IV for through-
8	Rosette Arm III-45°	Tension-Outside	34.5	4.4	thickness stress distribution in addition to longitudinal
9	Rosette Arm III-90°	Tension-Outside	34.5	4.4	
10	Rosette Arm IV-0°	Tension-Inside	34.5	4.4	
11	Rosette Arm IV-45°	Tension-Inside	34.5	4.4	
12	Rosette Arm IV-90°	Tension-Inside	34.5	4.4	
13	Rosette Arm V-0°	Tension-Outside	24.5	5.02	For longitudinal stresses and in-plane shear stress
14	Rosette Arm V-45°	Tension-Outside	24.5	5.02	
15	Rosette Arm V-90°	Tension-Outside	24.5	5.02	
16	Scarf Joint I	Tension-Outside	14.5	5.8	
17	Scarf Joint I	Tension-Inside	14.5	5.8	Scarf joint gages may detect any debond or
18	Scarf Joint III	Tension-Outside	11.0	5.8	delaminations or any unusual stress level arising
19	Scarf Joint IV	Tension-Inside	11.0	5.8	from this joint configuration
20*	Stress Concentration	Tension-Outside	34.5	1.3	
21	Stress Concentration	Tension-Outside	24.5	1.7	Stress concentration gages correspond to 0°
22*	Stress Concentration	Tension-Outside	14.5	1.3	rosette gages to assess the stress rise associated
23	Stress Concentration	Tension-Outside	11.0	1.7	with the bolting detail gages with (*) are over
24*	Stress Concentration	Tension-Outside	24.5	8.7	bonded areas
25	Stress Concentration	Tension-Outside	34.5	7.05	
26	I-Section Flange Stress	Tension-Inside	35.8	1.3	For longitudinal stress distribution on HY-130 frame
27	I-Section Flange Stress	Tension-Inside	28.5	1.3	
28	I-Section Flange Stress	Tension-Inside	20.75	1.3	
29	Rosette Arm VI-0°	Compression-Outside	43.0	−3.9	Rosette for longitudinal stress distribution and
30	Rosette Arm VI-45°	Compression-Outside	43.0	−3.9	in-plane shear
31	Rosette Arm VI-90°	Compression-Outside	43.0	−3.9	
32	Rosette Arm VII-0°	Compression-Outside	34.5	−4.4	Rosette VII located over Rosette VIII for through-
33	Rosette Arm VII-45°	Compression-Outside	34.5	−4.4	thickness stress distribution in addition to longitudinal
34	Rosette Arm VII-90°	Compression-Outside	34.5	−4.4	stresses and in-plane shear stresses
35	Rosette Arm VIII-0°	Compression-Inside	34.5	−4.4	
36	Rosette Arm VIII-45°	Compression-Inside	34.5	−4.4	
37	Rosette Arm VIII-90°	Compression-Inside	34.5	−4.4	
38	Rosette Arm IX-0°	Compression-Outside	24.5	−5.0	Rosette for longitudinal stresses and in-plane shear
39	Rosette Arm IX-45°	Compression-Outside	24.5	−5.0	
40	Rosette Arm IX-90°	Compression-Outside	24.5	−5.0	
41	Scarf Joint V	Compression-Outside	14.0	−5.8	Gages may indicate debond or delamination
42	Scarf Joint VI	Compression-Inside	14.0	−5.8	
43	Scarf Joint VII	Compression-Outside	14.0	−5.8	
44	Scarf Joint VII	Compression-Inside	14.0	−5.8	
45*	Stress Concentration	Compression-Outside	34.5	−1.3	Gages with (*) are over bonded areas
46	Stress Concentration	Compression-Outside	24.5	−1.7	
47*	Stress Concentration	Compression-Outside	14.5	−1.3	
48	Stress Concentration	Compression-Outside	11.0	−1.7	
49*	Stress Concentration	Compression-Outside	24.5	−8.7	
50	Stress Concentration	Compression-Outside	34.5	−7.05	

areas that posed problems for ultrasonic testing (UT): the scarf joint, the bolted and bonded joint between the composite skins and the steel spars, and the load application area. The NRL obtained results that were consistant with the McDonnell Douglas nondestructive evaluation.

The box beam was then sent to DTNSRDC for static and cyclic testing. The test setup and the loading apparatus used for the box beam are shown in Figure 4. The original apparatus included a bolt threaded into the box beam to prevent slippage of the loading ram, as well as a lock nut drawn against the load plates in an attempt to spread the load over as large an area as possible. After the first test series, delaminations were produced between the central steel loading plate (containing threaded hole) and the inner surface of the composite skin which was bonded to the central loading plate. The cause of delamination was thought to be, in part, a result of the method in which the load was applied (i.e., through-the-threaded hole in the steel central loading plate), whereby high normal tensile stresses were introduced. To eliminate this problem in subsequent tests, the female threads in the central steel loading plate were removed so that, during subsequent tests, all the load was applied to the box beam through the lock-nut arrangement.

The box beam was loaded statically in discrete increments; see Table 3. At each load increment, static measurements of deflection and strain were taken. Deflections were measured at the point of load application using a 5000 ohm, 6-in. potentiometer and an 8100A digital multimeter. Strain gage data were recorded using Gilmore Modular Graphic Plotters (Model 114J).

Nondestructive evaluation (pulse-echo ultrasonics) of the box beam was conducted by NRL prior to each test and following each subsequent failure. The results of the static tests and nondestructive evaluations are included in the following sections.

Results of Structure and Nondestructive Tests

The tests performed on Box Beam 1 are summarized in Table 4. As noted therein, following test 1 run 2, all subsequent tests were on the box beam which contained internal delaminations. As described later, attempts to repair these delaminations without removing the hybrid composite skins from the steel substructure were unsuccessful. The load-deflection data for Box Beam 1 corresponding to various tests are summarized in Table 3, and are also plotted in Figure 5.

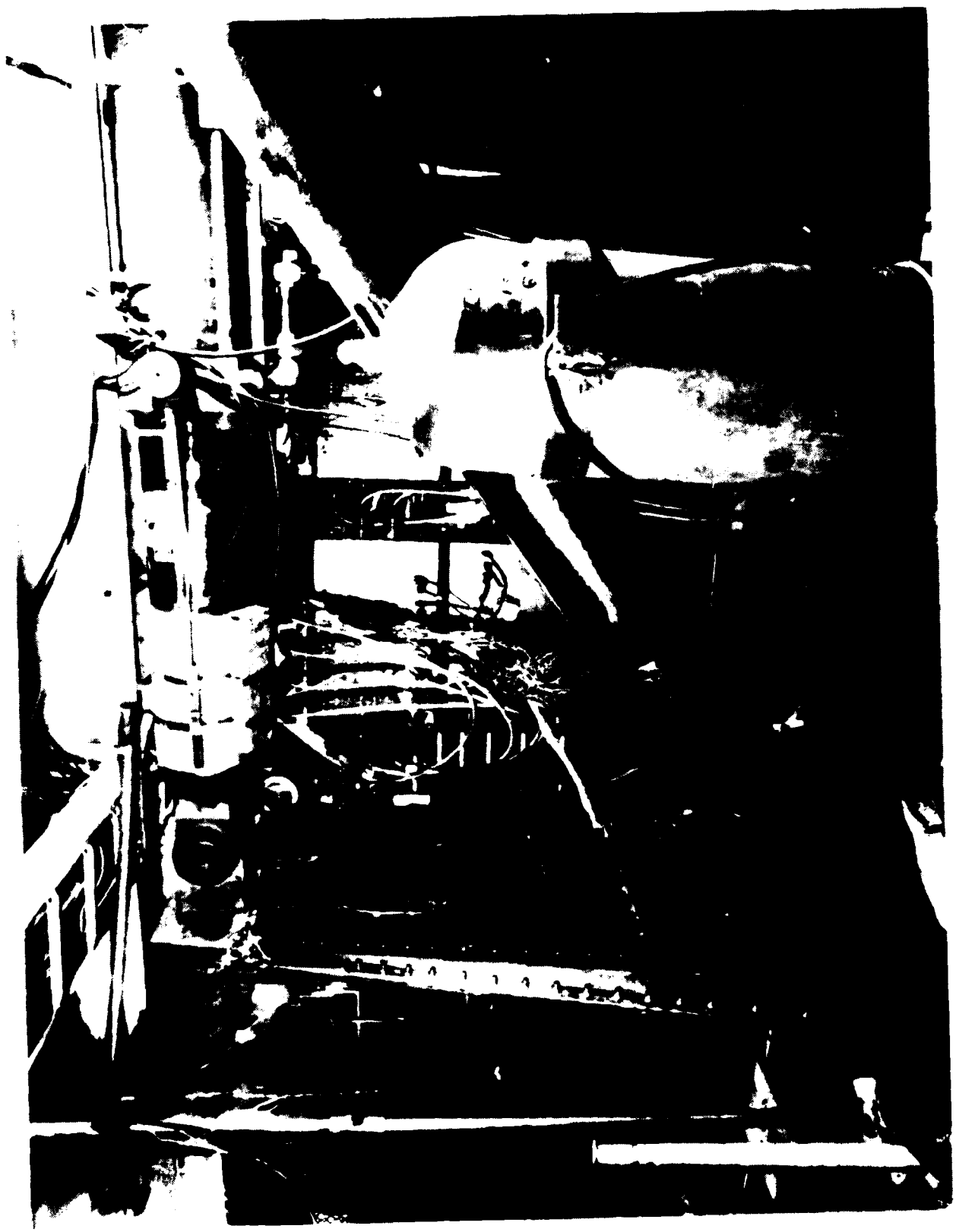

Figure 4 - Loading Apparatus

TABLE 3 - BOX BEAM 1: LOADING SCHEDULE AND DEFLECTIONS

Load in (kips)	Deflections (in.)								
	Test 1		Test 2		Test 3	Test 4	Test 5	Test 6	Test 7
	Run 1 8-7-78	Run 2 8-8-78	Run 3 1-9-79	Run 4 1-10-79	Run 5 1-26-79	Run 6 2-4-81	Run 7 3-2-81	Run 8 3-11-81	Run 9 3-12-81
0	0.004	0.005	0.000	0.000	0.000	0.000	0.000	0.000	0.000
3					0.100				
6	0.208	0.209	0.220	0.214	0.213	0.208	0.244		
9					0.323				
10								0.425	0.445
12	0.415	0.421	0.427	0.420	0.433	0.381	0.514		
15					0.542				
18	0.627	0.631	0.630	0.628	0.654	0.594	0.713		
20								0.832	0.882
21					0.763				
24	0.833	0.835	0.843	0.837	0.877	0.838	1.012		
27					0.993				
30	1.044	1.044	1.052	1.044	1.104	1.110	1.211	1.200	1.256
33					1.199				
36		1.255		1.264		1.312	1.453		
39						1.422			
40								1.619	1.689
42		1.461		1.475		1.611	1.705		
45						1.666			1.910
48		1.756				1.780	2.011		
50								2.030	2.127
51						1.925	2.005		
52								2.118	
54						2.108	—		
55									2.357
57						2.280	—	2.335	2.449
60						2.376			
52									2.280
48						2.000	—		
42									1.863
36						1.581	1.539		
25								1.093	
24	0.850		0.867		0.908	1.043	1.048		
18	0.645		0.665		0.693				
12	0.434	0.450	0.454		0.473	0.610	0.547		
6	0.220		0.250		0.250				
0	0.008	0.045	0.022		0.012	0.066	0.119	0.078	0.080
− 6	−0.232		−0.199		−0.240		−0.190		
−10								−0.422	−0.098
−12	−0.455		−0.414		−0.470	−0.444	−0.424		
−18						−0.619	−0.671		
−20								−0.824	−0.823
−24						−0.928	−0.908		
−25								−1.028	−1.041
−30						−1.189	−1.165		
−18						−0.722	−0.703		
− 6	−0.243		−0.214		−0.262	−0.258	−0.246		
0	−0.004		0.003		0.021	−0.027	−0.005	−0.020	−0.076

TABLE 4 - TESTS PERFORMED ON BOX BEAM 1

Test Number	Run Number	Maximum Applied Load (kips)	Remarks
1	1	30	No Damage.
	2	48	Delaminations; test stopped at 48 kips.
2	3	30	Delaminations of outer surface repaired. Delaminations on inner surface still present. Load stopped at 30 kips.
	4	48	Delaminations on outer surfaces; load stopped at 48 kips.
3	5	30	Damaged material on outer surfaces removed and replaced with new material. Delaminations on inner surface still present. Load stopped at 30 kips.
4	6	60	Box beam tested to design load. Delaminations on inner surface present before testing. Additional delaminations on outer surfaces as a result of test.
5	7	57	Test of box beam to maximum operating load with delaminations.
6	8	57	Test of box beam to maximum operating load after 10,000 fatigue cycles.
7	9	57	Test of box beam to maximum operating load after 17,000 fatigue cycles.

Table 5 gives the average strain sensitivities (μ in./in./kip load). For those locations where rosettes were applied, the strain data can be converted to equivalent laminate stresses using the equations for orthotropic materials[6,7] and the material properties given in Table 1. These stress values are presented in Table 6.

The box beam incurred delaminations to the inner surface of the tensile skin in the load application area at 48 kips (80 percent of the maximum operating load of 60 kips) during the second run of the first test. Figure 6 is a sketch showing the delaminated area as determined by NRL ultrasonic inspection (UT). The box beam was then shipped back to the manufacturer to be repaired. The repair consisted of: (1) bonding the outer four plies back to the tensile skin, (2) attempting to infiltrate resin into the delamination on the inner surface of the tensile skin, (3) bolting

TABLE 5 - EXPERIMENTAL STRAINS PER KIP LOAD FOR BOX BEAM 1

Strain Gage	Strain Sensitivities (μ in./in./kip)								
	Test 1		Test 2		Test 3 Run 5	Test 4 Run 6	Test 5 Run 7	Test 6 Run 8	Test 7 Run 9
	Run 1	Run 2	Run 3	Run 4					
1	33.3	35.7	–	–	–	–	–	–	
2	5.0	5.2	–	–	–	–	–	–	–
3	−31.7	−31.4	–	–	–	–	–	–	–
4	47.3	47.9	48.7	48.3	51.3	–	–	–	–
5	11.7	11.4	10.7	9.0	16.3	–	–	–	–
6	−34.0	−35.2	−31.0	−31.3	−30.0	–	–	–	–
7	56.0	55.7	56.7	57.0	57.3	56.0	57.0	57.6	60.0
8	13.0	13.1	13.3	13.3	15.7	14.0	10.0	8.2	7.2
9	−38.0	−40.7	−40.0	−40.7	−40.3	−42.7	−47.0	−50.0	−53.0
10	39.7	37.9	40.7	40.0	40.0	43.0	37.6	37.0	39.6
11	4.3	6.2	5.3	6.0	6.3	8.7	7.7	6.2	6.4
12	−33.7	−31.9	−33.0	−32.7	−34.0	−26.0	−30.3	−31.0	−27.6
13	54.7	55.5	56.0	56.3	56.8	–	–	–	–
14	15.7	15.0	16.3	14.0	16.0	–	–	–	–
15	−39.7	−41.2	−39.7	−40.0	−40.3	−42.0	−47.6	−49.4	−51.4
16	46.7	47.1	48.0	48.3	49.3	54.0	49.0	51.2	52.0
17	39.7	40.7	41.0	41.0	42.7	39.0	40.0	40.2	41.0
18	34.7	34.8	34.7	35.7	36.3	38.3	39.0	37.6	37.0
19	28.7	29.5	29.7	30.0	31.7	–	–	–	–
20	60.0	59.8	62.0	62.0	62.7	61.7	65.0	65.0	65.2
21	56.7	57.6	58.0	58.3	59.3	–	–	–	–
22	53.3	53.6	55.0	54.7	56.3	52.3	58.0	59.0	60.0
23	36.7	36.9	38.0	37.3	39.5	33.3	36.7	37.0	37.0
24	54.0	54.0	54.7	55.0	56.3	56.7	55.0	56.4	58.6
25	55.7	55.2	55.7	56.3	57.3	62.0	57.3	59.0	58.2

TABLE 5 - (Continued)

Strain Gage	Strain Sensitivities (μ in./in./kip)								
	Test 1		Test 2		Test 3 Run 5	Test 4 Run 6	Test 5 Run 7	Test 6 Run 8	Test 7 Run 9
	Run 1	Run 2	Run 3	Run 4					
26	26.7	27.4	29.3	29.7	32.3	31.7	31.0	31.8	35.6
27	30.3	30.7	31.7	31.7	32.7	24.7	38.0	32.6	37.0
28	29.7	30.2	32.0	32.0	33.0	24.0	25.7	30.2	32.4
29	−50.0	−48.8	−45.6	−45.3	—	—	—	—	—
30	−15.3	−15.2	− 9.3	− 7.7	—	—	—	—	—
31	29.7	29.3	28.0	29.0	—	—	—	—	—
32	−58.0	−57.6	−60.0	−59.0	−59.7	−59.3	—	—	—
33	−15.0	−15.7	−16.0	−15.0	−16.7	−16.0	—	—	—
34	37.3	35.7	38.0	36.7	36.3	31.3	—	—	—
35	−42.0	−41.7	−42.3	−41.3	−41.7	−42.0	−25.7	−47.0	42.6
36	− 5.0	− 4.3	− 2.3	− 3.0	− 3.7	− 3.3	−11.7	−11.2	−11.4
37	38.7	39.3	39.0	41.7	39.0	43.3	—	—	—
38	−56.7	−55.7	−56.7	−55.3	−57.0	−56.0	—	—	—
39	−11.0	−11.2	−10.3	− 9.7	−11.3	−10.0	—	—	—
40	36.0	33.8	35.0	35.7	36.3	36.7	34.7	—	—
41	−48.7	−49.0	−49.0	−47.6	−49.8	—	—	—	—
42	−40.3	−40.0	−37.7	—	—	−32.3	−32.7	−33.0	32.8
43	−37.0	−36.9	−36.3	−35.3	−37.7	—	—	—	—
44	−29.0	−28.6	−29.0	−28.0	−30.0	−27.3	−28.0	−27.2	28.0
45	−60.3	−59.8	−60.7	−61.3	−63.3	−64.7	—	—	—
46	−59.3	−59.3	−59.3	−59.3	−60.7	−60.0	—	—	—
47	−51.7	−51.7	−47.6	−50.3	−51.7	−51.7	—	—	—
48	−39.3	−38.8	−39.3	−39.0	−40.3	−40.0	—	—	—
49	−57.7	−56.9	−58.0	−58.0	−58.3	−54.0	—	—	—
50	—	—	−58.7	−58.7	−59.7	−58.3	—	—	—

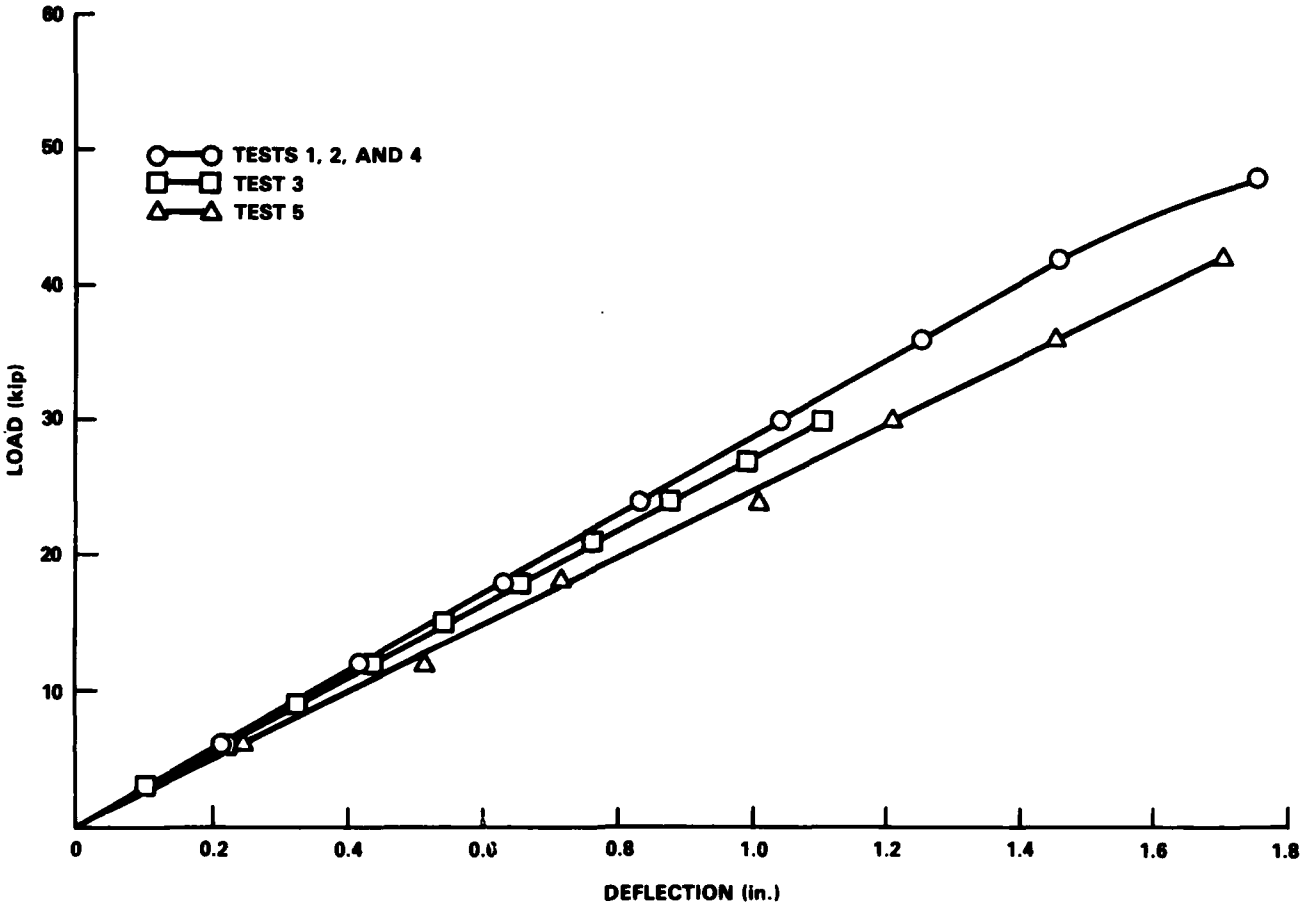

Figure 5 - Box Beam 1 Static Deflection Behavior

and bonding 0.5-in. thick steel doubler plates to the load application area, and (4) bonding a layer of glass-reinforced plastic to the edges of both skins. Figure 7 shows the location of the doubler plates as well as the results of the NRL UT following the attempted repair. (The internal aluminum blocks were used to minimize the volume of resin used during infiltration so as to prolong the pot life.) The initial interpretation of the NRL UT results indicated that the delamination still existed; i.e., the attempt to infiltrate the internal delaminations may have been unsuccessful. However, futher studies related to the effect of thick bonds showed that the ultrasonic signal could have been caused by a delamination or a thick layer of resin. Thus, the adequacy of the repair could not be determined.

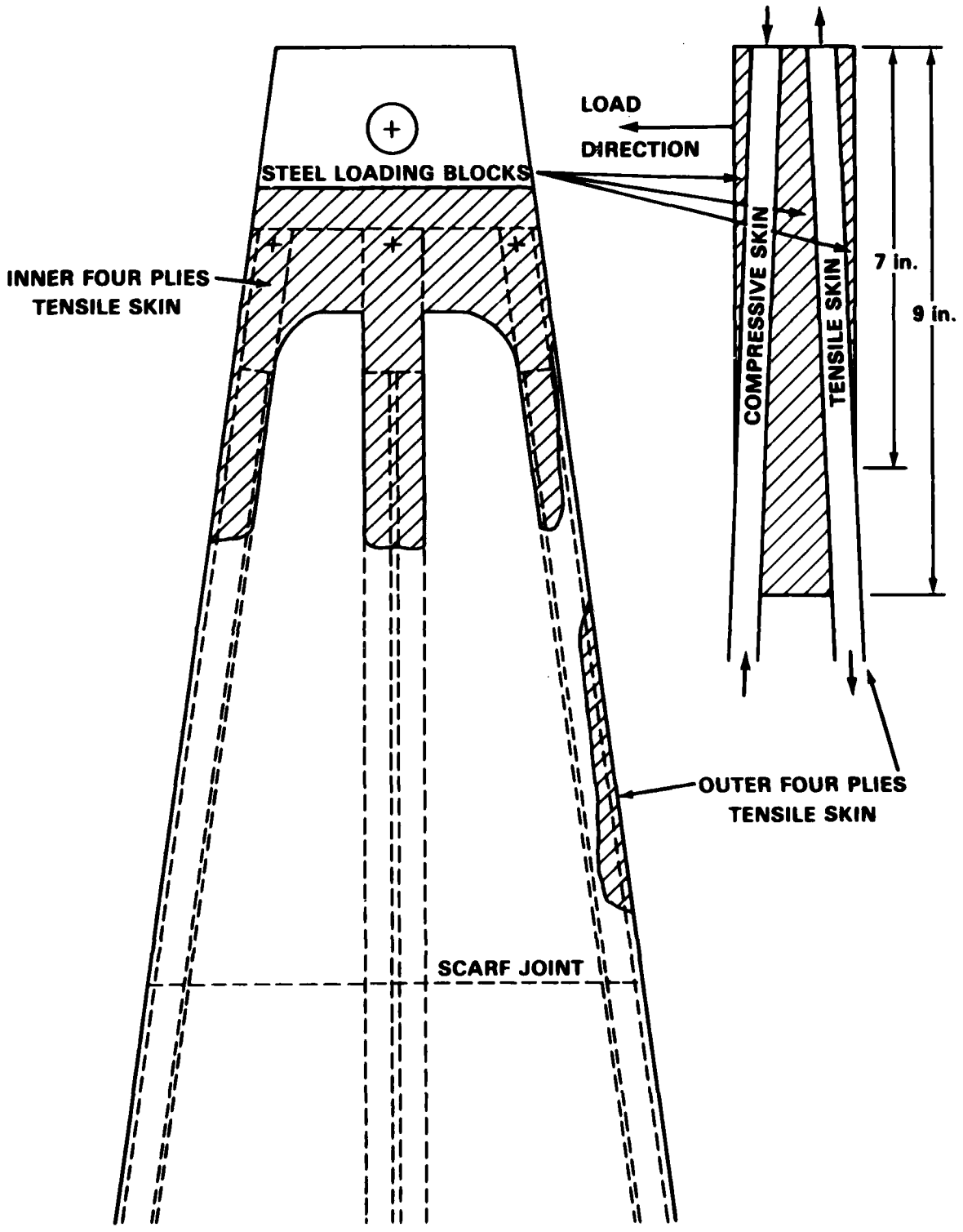

Figure 6 - Sketch of Delaminations Found by UT Following Test 1

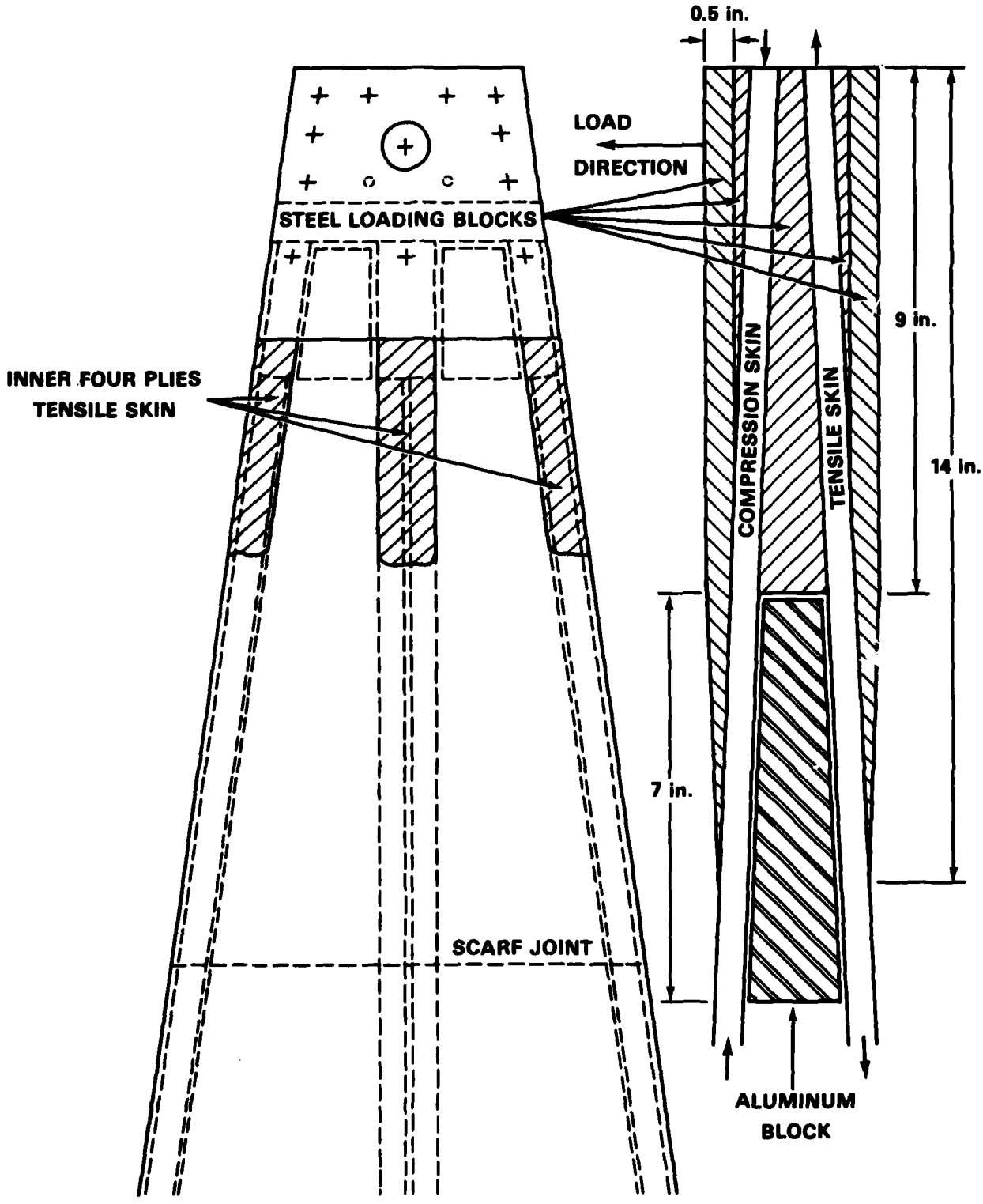

Figure 7 - Sketch of Delaminations Found by UT Following Repair 1

TABLE 6 - EXPERIMENTAL STRESSES PER KIP LOAD FOR BOX BEAM 1

Rosette Location	Stress Direction	Strain Sensitivities (psi/kip)								
		Test 1		Test 2		Test 3 Run 5	Test 4 Run 6	Test 5 Run 7	Test 6 Run 8	Test 7 Run 9
		Run 1	Run 2	Run 3	Run 4					
1-3	σ_L	410	450							
	σ_T	- 32	- 21							
4-6	σ_L	626	631	660	652	705				
	σ_T	11	8	32	29	48				
7-9	σ_L	750	734	753	755	761	731	730	728	755
	σ_T	25	10	18	15	18	1	- 17	- 30	- 36
10-12	σ_L	505	483	524	514	509	588	485	472	527
	σ_T	- 18	- 15	- 9	- 11	- 17	36	- 8	- 14	14
13-15	σ_L	722	729	743	747	753				
	σ_T	11	7	16	16	16				
29-31	σ_L	-602	-586	-546	-539					
	σ_T	- 9	- 8	- 4	1					
32-34	σ_L	-690	-675	-715	-691	-716	-726			
	σ_T	2	- 4	0	- 3	- 7	- 30			
35-37	σ_L	-465	-459	-468	-446	-460	-451			
	σ_T	57	60	57	73	59	78			
38-40	σ_L	-676	-668	-678	-657	-679	-664			
	σ_T	0	- 7	- 4	3	1	6			

A second static test was conducted, and again the box beam delaminated in the load application area at 48 kips during the second run as shown in Figure 8; this time the delaminations were much more extensive. The box beam was then tested to 30 kips to determine what effect the delamination had on the overall stiffness; it was sent back to the manufacturer for repairs. This time the repairs included removing the doubler plates and outer delaminated plies from both skins, replacing them with a built-up area, as shown in Figure 9, and bolting (only) the outermost 0.5-in. thick steel doubler plates back in place. Following the second repair, the

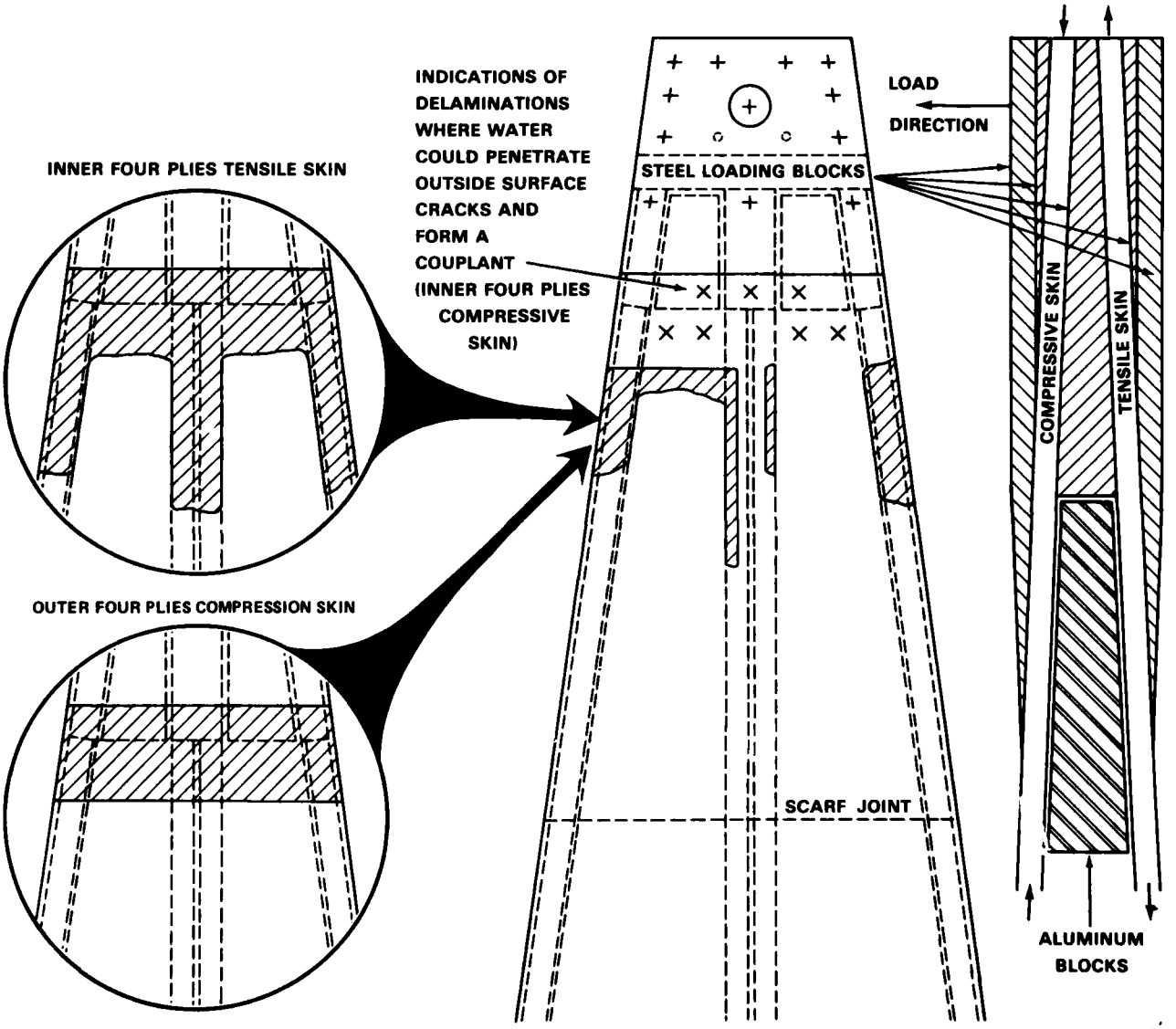

Figure 8 - Sketches of Delaminations found by UT Following Test 2

box beam was inspected by NRL using a hand scan UT technique and by the Sea Water Component Integrity Measuring Instrument[5] (SCIMI) developed for the Navy by the Electric Boat Division of General Dynamics. The results of this inspection indicated that there were still delaminations on the inside surface of both skins along the spars, and potential midskin delaminations just above the scarf joint in both skins. There was also an indication of delaminations on the outside surface of the built-up areas on both skins in the load application area.

Following the second repair, the box beam was again tested statically; this time to the maximum planned operating load of 60 kips. The box beam sustained 60 kips for 5 min. Several surface delaminations occurred during this test run. The strain data were analyzed and an exact maximum load of 57 kips was selected for the cyclic tests. At 57 kips, the maximum stress in the box beam was 43 ksi. This leads to a design safety factor of 1.58 with an ultimate strength allowable of 68 ksi. The box beam was then loaded to a maximum load of 57 kips prior to the initiation of the cyclic tests. Extensive delamination occurred during the fourth test in the outer layers of both skins. This limited the effectiveness of the UT inspection, and made the SCIMI inspection unproductive. The NRL hand scan UT inspections did find evidence of internal delaminations in the built-up section of the load application area, but no growth of previously noted flaws could be detected.

BOX BEAM 2

Further Analytical Investigations

Prior to testing Box Beam 2, a limited analytical effort was undertaken to establish possible causes and modes of failure in Box Beam 1.

McDonnell Douglas attributed the first failure in the loading plate region to a combination of interlaminar shear stress due to the free edge effect, and normal tension caused by the application of load through a threaded joint in the central portion of the steel loading plate. The internal delaminations in the tensile skin (see Figure 6) were believed to have been caused by the "lap joint" effect. Numerical calculations supporting the latter hypothesis are given in Appendix A.

To establish the cause of delaminations in a rigorous manner, Virginia Polytechnic Institute and State University (Virginia Tech) was contracted to perform a three-dimensional, elastic, finite element analysis of the box beam using the SAP 4

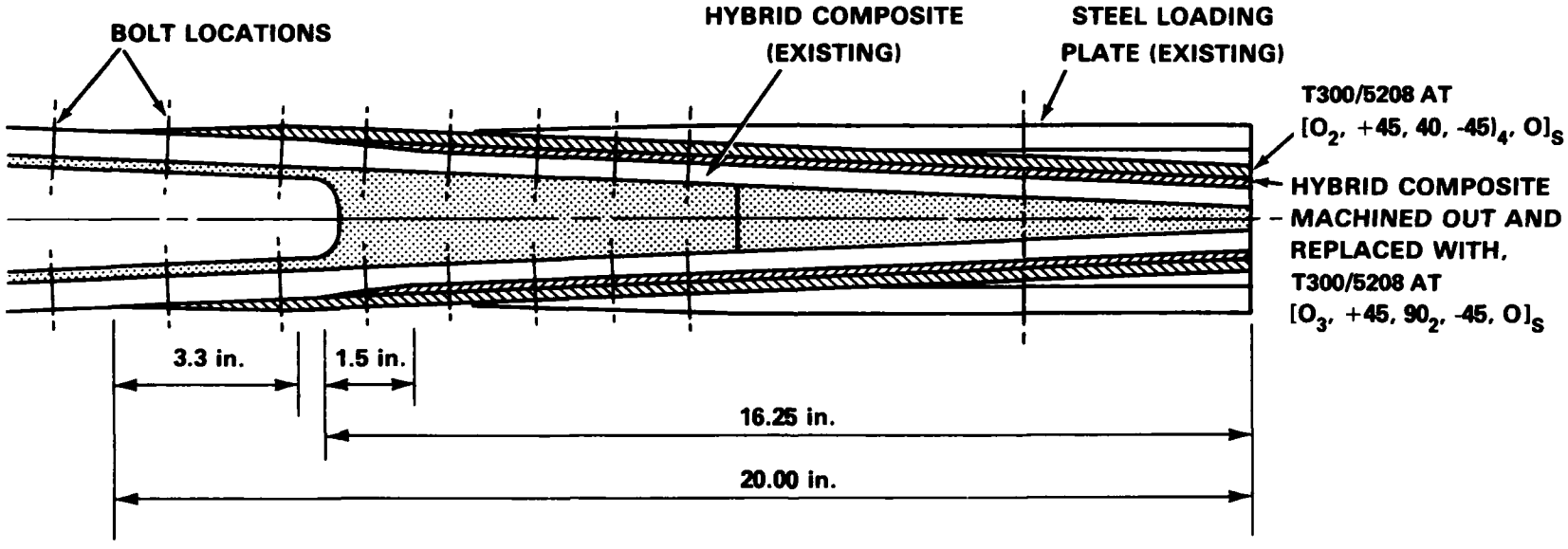

Figure 9 - Box Beam Loading Area Showing Results of Repair 2

computer code. The finite element analysis is briefly described in Appendix B. The surface stresses obtained from the SAP 4 analysis agreed neither with the NASTRAN results nor with the results obtained from the strength of materials analyses (both of which showed good correlation with the test data). Because of this disagreement, the reliability of the SAP 4 results seemed questionable. While the SAP 4 results were not able to predict the failure load or the mode of failure, they did point out areas of concern.

Since the delaminations were believed to have been the result of high interlaminar shear stresses, an attempt was made to modify the manner in which the load was applied so as to reduce the shear stress. This was thought possible by moving the point of load application. Appendix C summarizes the results of varying the point of load application and magnitude of load on the stress distribution. Since moving the load application point did not look too promising, it was decided to maintain the original loading method.

Description of Test Procedures

To obtain further insight into the mode of failure, Box Beam 2 was instrumented with additional strain gages on the laminate skin (Figure 10) at finite element centers and on the laminate edges (Figure 11). In addition, photoelastic material was applied to the laminate edges as shown in Figure 12. In order to prevent delaminations similar to those that occurred in Box Beam 1, the maximum load applied to Box Beam 2 was restricted to 30 kips. It was loaded in two runs consisting of several increments as shown in Table 7.

Results of Structural and Nondestructive Tests

Tables 8 and 9 give the strain sensitivities and average stress values, respectively, for the manufacturer's gages. Deflection data are included in Table 7. The strain sensitivities for DTNSRDC gages are given in Table 10 and corresponding average stress values are given in Table 11. Shear stresses, obtained from the photoelastic material and shear rosettes, are given in Table 12. Figure 13 displays a qualitiative indication of the distribution of the shear stress magnitudes obtained from the photoelastic material.

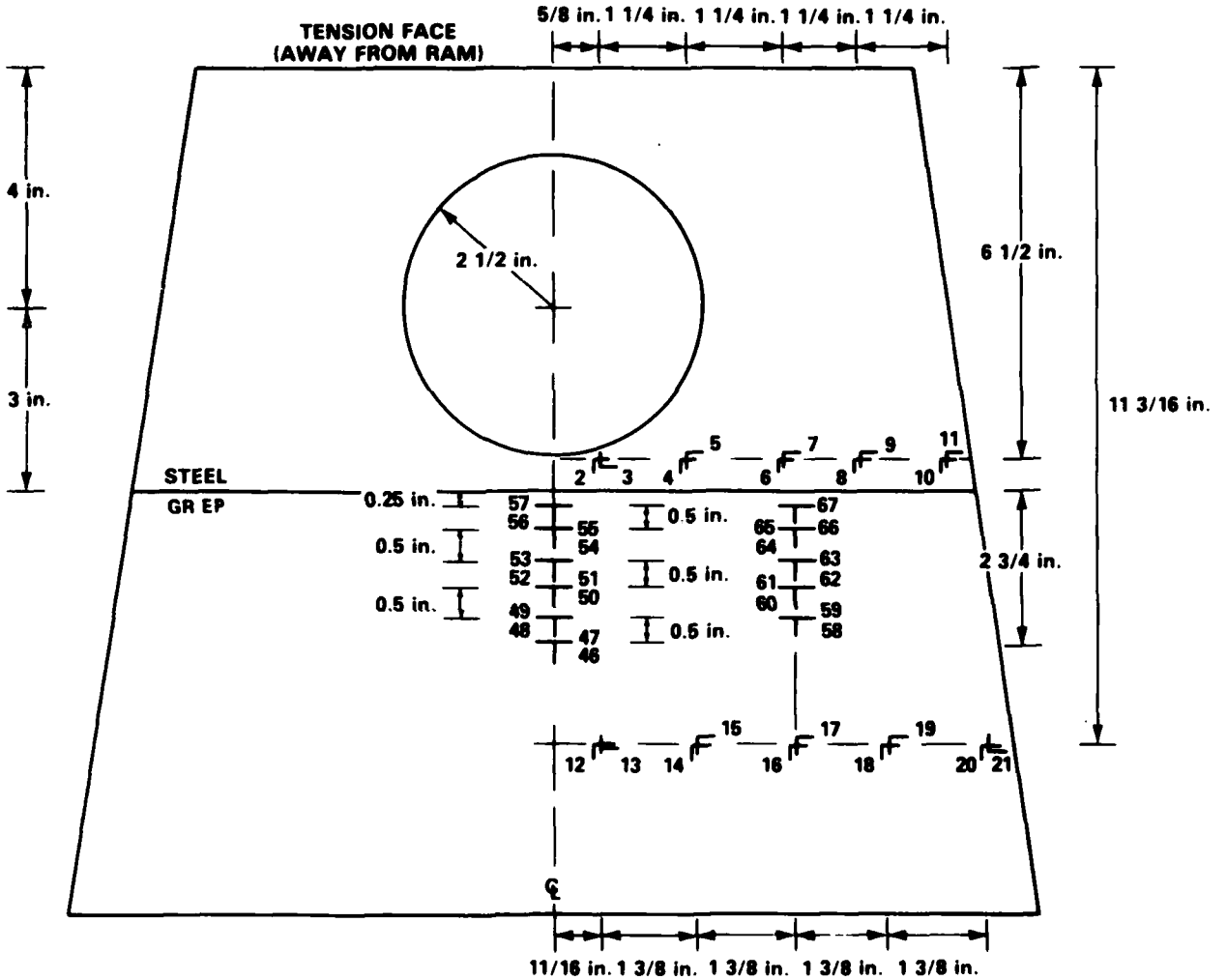

Figure 10 - DTNSRDC Strain Gage Locations for Box Beam 2: Laminate Surface

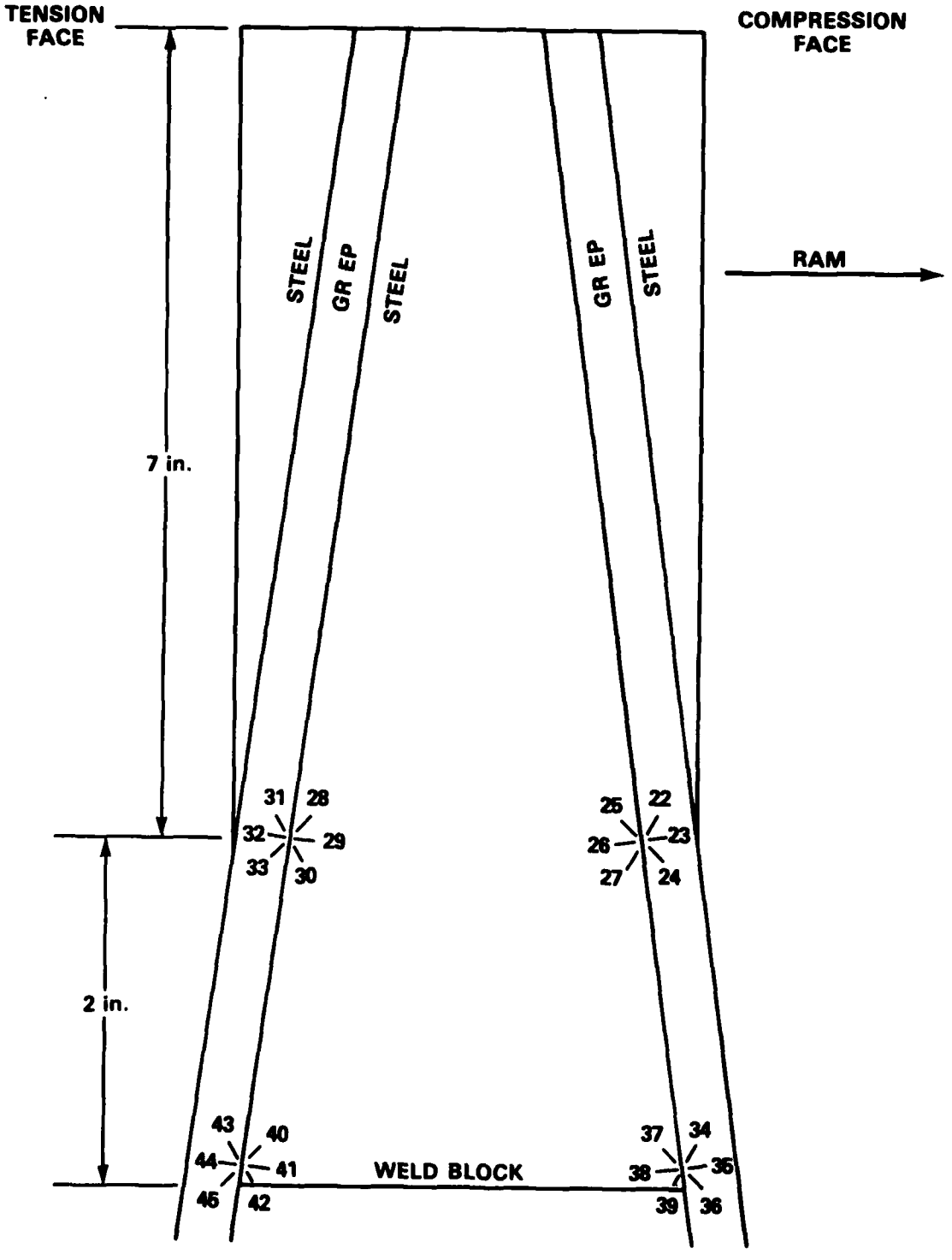

Figure 11 - DTNSRDC Strain Gage Locations for Box Beam 2: Laminate Edges

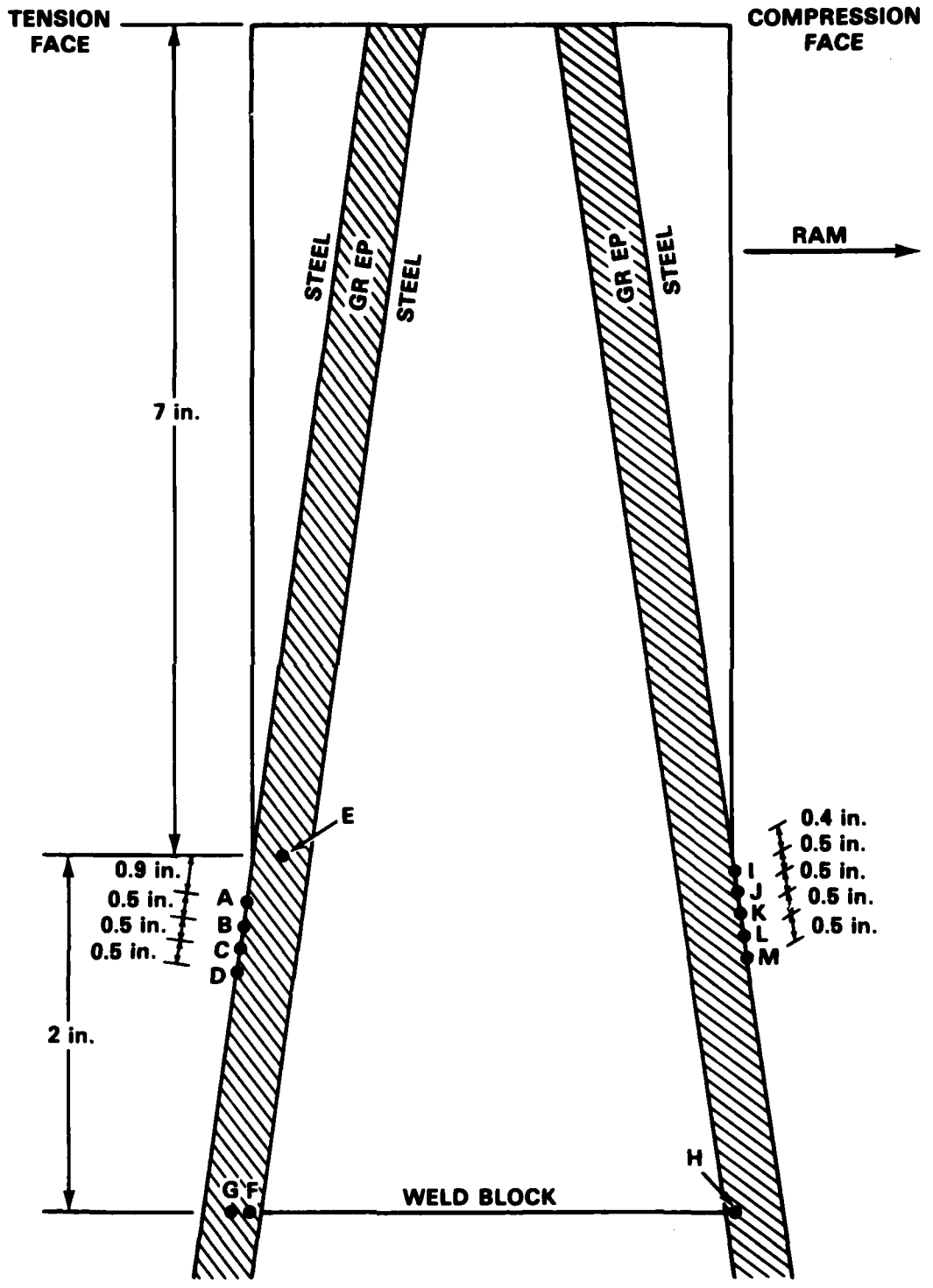

Figure 12 - Location of Photoelastic Material and Shear Stress Points

TABLE 7 - BOX BEAM 2: LOADING SCHEDULE AND DEFLECTIONS

Load (kips)	Deflection (in.)					
	Test 1		Test 2	Test 3	Test 4	Test 5
	Run 1 5-6-80	Run 2 5-7-80	Run 3 5-1-81	Run 4 5-4-81	Run 5 5-12-81	Run 6 6-5-81
0	0	0	0	0	0	0
5	0.167	0.160	0.159	0.181	0.178	0.225
10	0.337	0.337	0.350	0.379	0.383	
15	0.506	0.509	0.494	0.538	0.549	0.643
20	0.661	0.677	0.682	0.736	0.744	
25	0.823	0.835	0.823	0.869	0.878	1.037
30	0.985	0.995	1.007	1.053	1.074	
35			1.154	1.216	1.245	1.457
42			1.387	1.474	1.510	1.748
30						1.303
25	0.855	0.845				0.898
20	0.693	0.684				0.525
15	0.525	0.522				
10	0.354	0.347				
5	0.184	0.168				
0	0.007	−0.018	0	0	0	0
− 5	−0.163	−0.196	−0.191	−0.189	—	
−10	−0.328	−0.367	−0.339	−0.361	—	−0.446
−15	−0.499	−0.541	−0.507	−0.561	—	
−20			−0.624	−0.747	—	−0.869
−25			−0.788	−0.918	—	−1.070
−15						−0.680
−10	−0.364	−0.368				
− 5	−0.189	−0.202				−0.283
0	−0.008	−0.017	0	0	—	−0.073

TABLE 8 - EXPERIMENTAL STRAINS PER KIP LOAD FOR BOX BEAM 2; CONTRACTOR GAGES

Strain Gage	Strain Sensitivities (μ in./in./kip)					
	Test 1		Test 2	Test 3	Test 4	Test 5
	Run 1	Run 2	Run 3	Run 4	Run 5	Run 6
1	36.4	35.0	36.6	35.9	35.0	29.2
2	0.7	0.8	3.1	2.6	0.0	0.0
3	−32.0	−32.0	−31.0	−31.0	−32.0	−28.0
4	48.0	50.0	—	—	—	—
5	10.0	11.4	12.4	12.4	9.5	7.0
6	−32.0	−35.0	−32.3	−32.8	−33.0	−35.6
7	56.7	57.1	57.7	57.7	58.0	57.6
8	13.3	13.3	14.4	13.9	12.5	11.7
9	−40.0	−40.0	−41.0	−41.8	−41.5	−44.7
10	41.3	40.0	47.2	41.7	42.5	37.2
11	6.3	7.3	6.8	6.9	5.5	5.5
12	−31.1	−30.0	−33.8	−33.2	−33.0	−25.6
13	56.0	56.0	58.4	57.9	58.0	59.5
14	12.0	13.3	14.2	13.7	12.5	11.5
15	−42.4	−40.0	−40.1	−40.6	−42.0	−46.0
16	50.0	50.0	49.0	49.5	50.0	50.5
17	40.0	42.7	42.7	43.7	44.5	44.4
18	36.7	40.0	38.6	38.7	38.5	39.5
19	32.0	32.0	32.1	32.4	33.5	33.5
20	60.0	60.0	61.2	61.6	61.5	72.1
21	61.3	60.0	57.0	59.6	60.0	60.0
22	54.0	50.0	53.3	56.9	57.0	57.0
23	42.1	40.0	40.9	41.1	41.0	40.0
24	56.0	54.1	57.2	57.8	58.0	59.0
25	56.0	60.0	58.1	59.0	59.0	57.7

TABLE 8 - (Continued)

Strain Gage	Strain Sensitivities (μ in./in./kip)					
	Test 1		Test 2 Run 3	Test 3 Run 4	Test 4 Run 5	Test 5 Run 6
	Run 1	Run 2				
26	26.7	26.7	27.1	26.8	26.5	36.0
27	30.0	30.1	31.4	30.7	31.0	44.4
28	32.0	32.0	32.7	30.9	31.0	33.5
29	−47.3	−48.0	−50.2	−50.3	−50.0	−61.5
30	−13.3	−13.3	−12.6	−12.6	−14.0	−14.0
31	28.6	28.6	30.4	30.7	30.0	38.6
32	−58.2	−60.0	−59.7	−60.2	−59.5	−62.0
33	−20.0	−20.0	—	—	—	—
34	35.0	36.0	38.2	38.1	37.5	39.5
35	−40.0	−42.0	−42.3	−42.1	−41.5	−41.5
36	− 2.0	− 2.2	− 2.8	− 1.4	− 4.0	0
37	41.5	40.0	40.2	39.8	39.0	41.7
38	−57.8	−57.1	−60.2	−58.4	−58.0	−58.0
39	−16.0	−18.2	—	—	—	—
40	36.0	36.0	—	—	—	—
41	−48.0	−51.4	−51.4	−50.9	−50.5	−50.0
42	−38.7	−40.0	−39.8	−41.0	−41.0	−40.5
43	−37.4	−40.0	−38.6	−38.3	−37.5	−38.0
44	−32.0	−32.0	−32.0	−32.5	−33.0	−32.5
45	−60.0	−60.0	−68.5	−63.4	−64.0	−67.5
46	−60.0	−60.0	−60.2	−61.4	−61.0	−60.5
47	−54.5	−55.0	−55.2	−54.3	−54.5	−54.0
48	−40.0	−40.0	−40.6	−40.1	−40.5	−40.5
49	−57.1	−57.1	−58.2	−58.4	−57.5	−57.0
50	−56.0	−56.0	−58.1	−58.1	−57.5	−60.0

TABLE 9 - EXPERIMENTAL STRESSES PER KIP LOAD FOR BOX BEAM 2: CONTRACTOR GAGES

Rosette Location	Stress Direction	Stress Sensitivities (psi/kip)					
		Test 1		Test 2 Run 3	Test 3 Run 4	Test 4 Run 5	Test 5 Run 6
		Run 1	Run 2				
1-3	σ_L	459	436	466	455	436	359
	σ_T	− 21	− 27	− 15	− 18	− 27	− 29
4-6	σ_L	645	665	—	—	—	—
	σ_T	24	17	—	—	—	—
7-9	σ_L	753	759	765	762	768	749
	σ_T	18	19	16	12	15	− 3
10-12	σ_L	541	524	625	539	553	496
	σ_T	3	3	12	− 6	− 2	15
13-15	σ_L	732	742	780	770	766	774
	σ_T	3	15	24	19	12	− 2
29-31	σ_L	−568	−578	−602	−603	−601	−734
	σ_T	− 7	− 9	− 7	− 6	− 8	− 2
32-34	σ_L	−699	−721	−711	−718	−710	−738
	σ_T	− 9	− 10	2	0	− 1	1
35-37	σ_L	−429	−461	−464	−463	−457	−449
	σ_T	76	63	63	62	60	72
38-40	σ_L	−691	−681	—	—	—	—
	σ_T	− 3	− 1	—	—	—	—

TABLE 10 - EXPERIMENTAL STRAINS PER KIP LOAD FOR BOX BEAM 2: DTNSRDC GAGES

Strain Gage	Strain Sensitivities (μ in./in./kip) Test 1 Run 1	Test 1 Run 2	Strain Gage	(μ in./in.) Test 1 Run 1	Test 1 Run 2	Strain Gage	/kip) Test 1 Run 1	Test 1 Run 2
2	13.3	13.3	28	8.0	8.0	56	21.8	22.0
3	−26.7	−26.7	29	− 2.2	− 2.2	57	−21.1	−21.6
			30	− 1.8	− 2.5			
4	14.5	16.0				58	35.2	35.2
5	−22.9	−24.0	31	−40.0	−36.4	59	−28.0	−30.4
			32	—	—			
6	13.3	14.5	33	44.0	45.7	60	33.6	33.6
7	−16.0	−16.0				61	−28.8	−28.8
			34	24.0	24.6			
8	16.0	16.0	35	6.7	7.3	62	31.2	32.0
9	−13.3	−13.3	36	−36.4	−36.0	63	−25.6	−25.6
10	13.3	13.3	37	− 8.6	− 8.0	64	28.8	28.8
11	−10.9	−10.0	38	− 0.4	− 0.4	65	−22.4	−23.2
			39	0.7	1.1			
12	33.3	33.3				66	25.6	28.0
13	− 8.9	−16.0	40	8.0	8.6	67	−20.8	−20.8
			41	− 0.7	− 0.4			
14	40.0	42.9	42	− 0.2	− 1.1			
15	−30.0	−30.0						
			43	−30.0	−30.0			
16	44.2	42.9	44	− 0.5	− 1.5			
17	−32.7	−34.7	45	48.9	50.0			
18	44.0	42.7	46	34.3	36.4			
19	−33.3	−36.4	47	−17.1	−17.1			
20	22.9	18.2	48	31.1	33.6			
21	−28.6	−28.6	49	−24.0	−23.2			
22	35.0	35.2	50	28.8	29.6			
23	—	7.2	51	−21.8	−22.4			
24	—	−41.6						
			52	25.6	24.0			
25	− 8.0	− 8.0	53	−22.2	−22.4			
26	1.3	2.0						
27	5.7	3.1	54	22.4	24.0			
			55	−22.9	−22.4			

TABLE 11 - EXPERIMENTAL STRESSES PER KIP LOAD FOR BOX BEAM 2: DTNSRDC GAGES

Strain Gage Location	Stress Direction	Stress Sensitivities in Test 1 (psi/kip)		Strain Gage Location	Stress Location	Test 1 (psi/kip)	
		Run 1	Run 2			Run 1	Run 2
2-3	σ_L	174	174	52-53	σ_L	324	297
	σ_T	−749	−749		σ_T	− 13	− 21
4-5	σ_L	252	290	54-55	σ_L	270	297
	σ_T	−612	−633		σ_T	− 29	− 20
6-7	σ_L	280	320	56-57	σ_L	267	268
	σ_T	−396	−384		σ_T	− 23	− 24
8-9	σ_L	396	396	58-59	σ_L	455	446
	σ_T	−280	−280		σ_T	− 5	− 17
10-11	σ_L	331	340	60-61	σ_L	426	426
	σ_T	−228	−198		σ_T	− 16	− 16
12-13	σ_L	500	471	62-63	σ_L	400	413
	σ_T	85	49		σ_T	− 9	− 6
14-15	σ_L	524	571	64-65	σ_L	374	371
	σ_T	3	15		σ_T	− 2	− 6
16-17	σ_L	581	552	66-67	σ_L	329	368
	σ_T	6	− 9		σ_T	6	3
18-19	σ_L	575	542				
	σ_T	2	− 18				
20-21	σ_L	255	180				
	σ_T	− 56	− 75				
46-47	σ_L	483	517				
	σ_T	47	55				
48-49	σ_L	405	448				
	σ_T	− 1	13				
50-51	σ_L	377	387				
	σ_T	1	1				

TABLE 12 - EXPERIMENTAL SHEAR STRESSES PER KIP LOAD FOR BOX BEAM 2: ROSETTES AND PHOTOELASTIC MEASUREMENTS

Strain	Shear Stress (psi/kip)	Photoelastic	Shear Stress (psi/kip)
22-24	54.0	A	12
31-33	—	B	48
34-36	44.8	C	37
43-45	56.5	D	38
		E	35
		F	35
		G	50
		H	−35
		I	−21
		J	−39
		K	−42
		L	−39
		M	−43

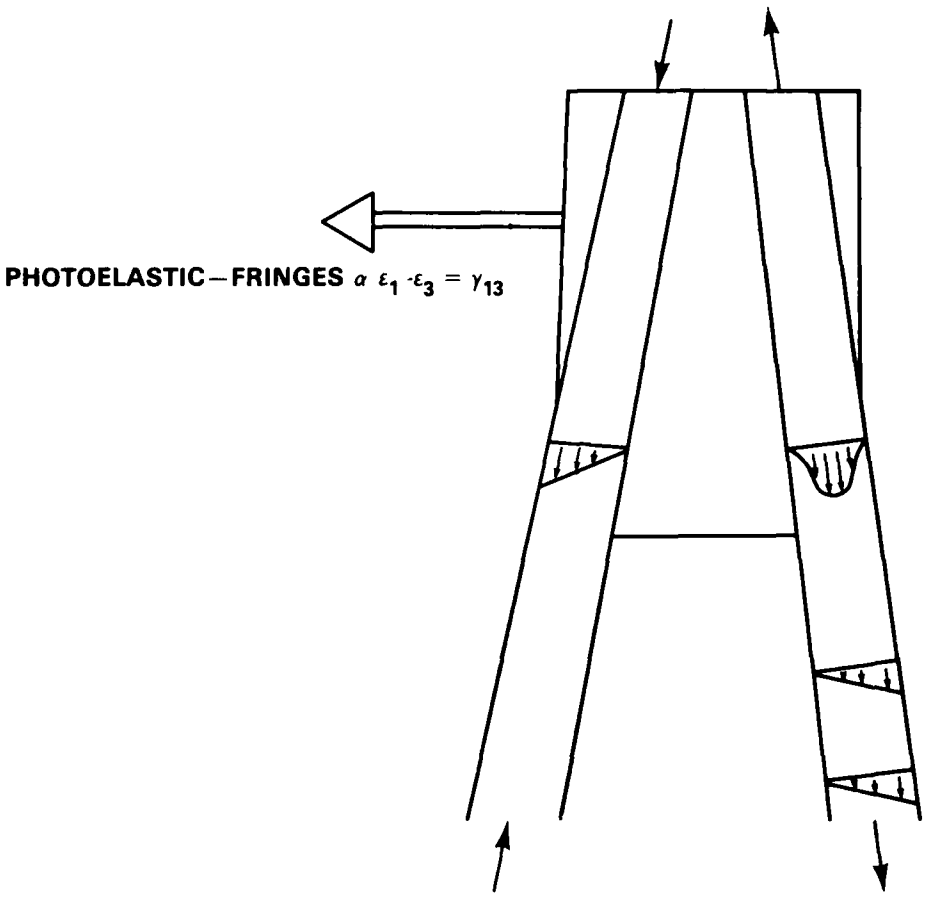

Figure 13 - Qualitative Distribution of Shear Stress Magnitude for Box Beam 2 from Photoelastic Measurements

Box Beam 2 was inspected by the manufacturer as described in a previous section, as well as by the NRL before and after the static test using the hand-scan and SCIMI UT techniques.[5] The NRL investigation reinforced the manufacturer's conclusions that no major delaminations, debonds, or anomalies existed in the skins or in the scarf joint regions. It should be pointed out that the SCIMI technique creates a permanent digital acoustic map through the thickness of the laminate. This is valuable for tracking the growth of known delaminations throughout the lifetime cyclic test of the box beams.

EVALUATION OF STATIC TEST RESULTS

Strain gage data and deflection data for both box beams were compared for all the static tests. Despite the delaminations of the inner and outer plies, the data were repeatable. (This excludes data from gages on the delaminated skins.) The additional surface gages on the second box beam were located at the points that corresponded to the NASTRAN finite element centers. The data obtained were compared to NASTRAN predictions and, as can be seen from Figures 14 through 19, most of the gage data were consistent with the analysis. The only discrepancy found was in the longitudinal stresses with respect to the transverse direction (σ_y versus y) on the steel plate. Deflection data for the various runs were consistent and agreed with the design analysis prediction. NASTRAN, however, predicted the box beam to be slightly more rigid than it actually was. There were minor changes in deflection (becoming less stiff) due to the delaminations.

The several attempts to determine interlaminar shear values were inconsistent and failed to indicate stresses sufficient to cause delamination (4.8-6.8 ksi). The SAP 4 three dimensional finite element analysis was unsuccessful. Although the values obtained by the photoelastic analysis are the principal shearing stresses, they may not be in the proper direction (parallel to the plane of the lamina). In addition, those values obtained using shear rosettes have been averaged across several plies (equal to the gage width). It was felt that one or both methods might indicate shear stress levels close to the interlaminar shear strength of the box beam laminate.

CYCLIC TESTS

BOX BEAM 1

Following the final static test to 57 kips and the attempted UT inspections by SCIMI and hand techniques, the box beam was tested cyclically using the spectrum shown in Figure 20. This spectrum included all the loading conditions that were used for the metallic box beams. The box beam sustained 19 blocks, or 19,000 cycles prior to catastrophic failure. The failed box beam is shown in Figure 21. Because the damage to the outer plies was of such an extensive magnitude during the static test to the maximum operating load, ultrasonic inspection of the box beam at selected intervals during the cyclic test was impossible. However, the cyclic test was halted

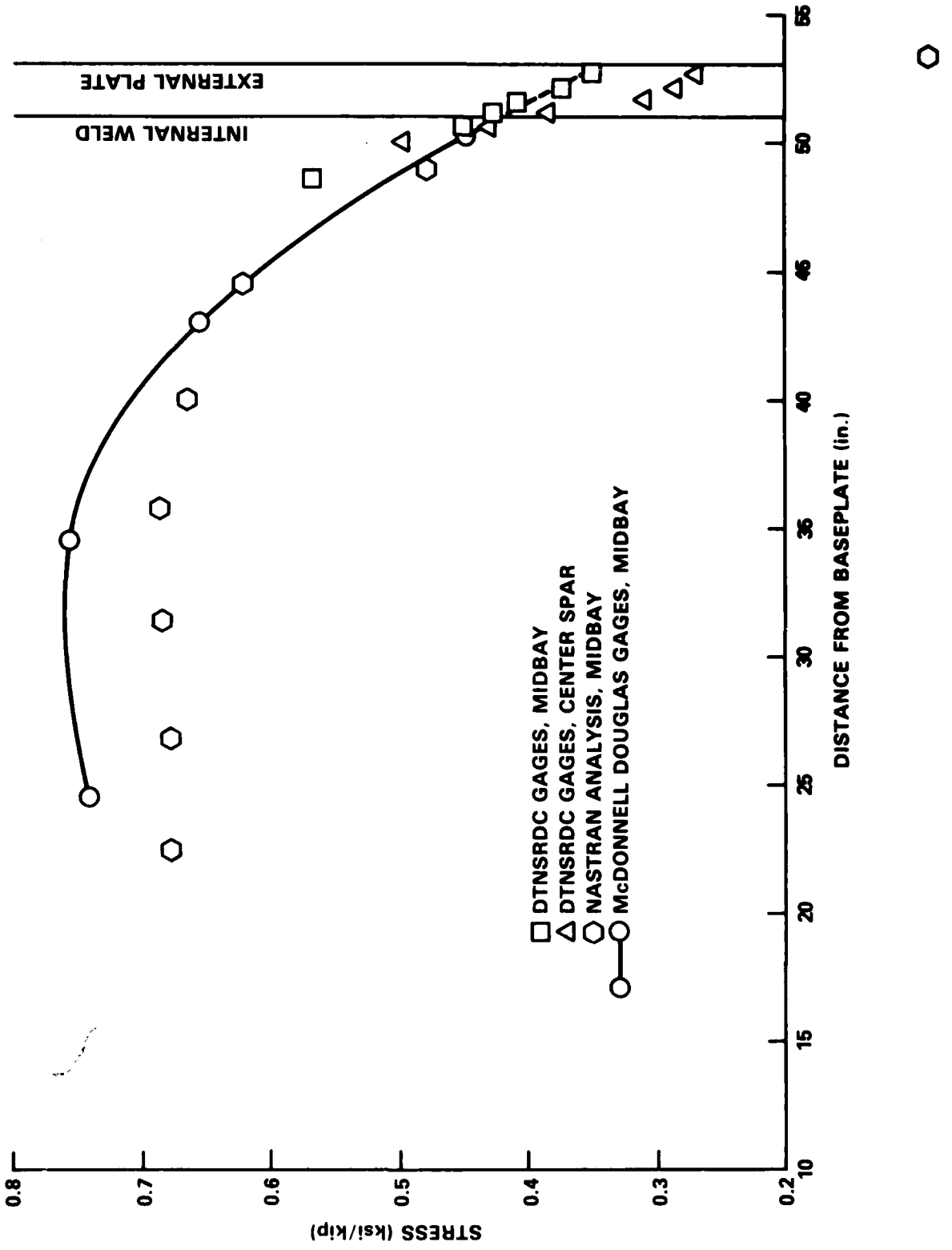

Figure 14 - Longitudinal Stress versus Longitudinal Distance Along Box Beam

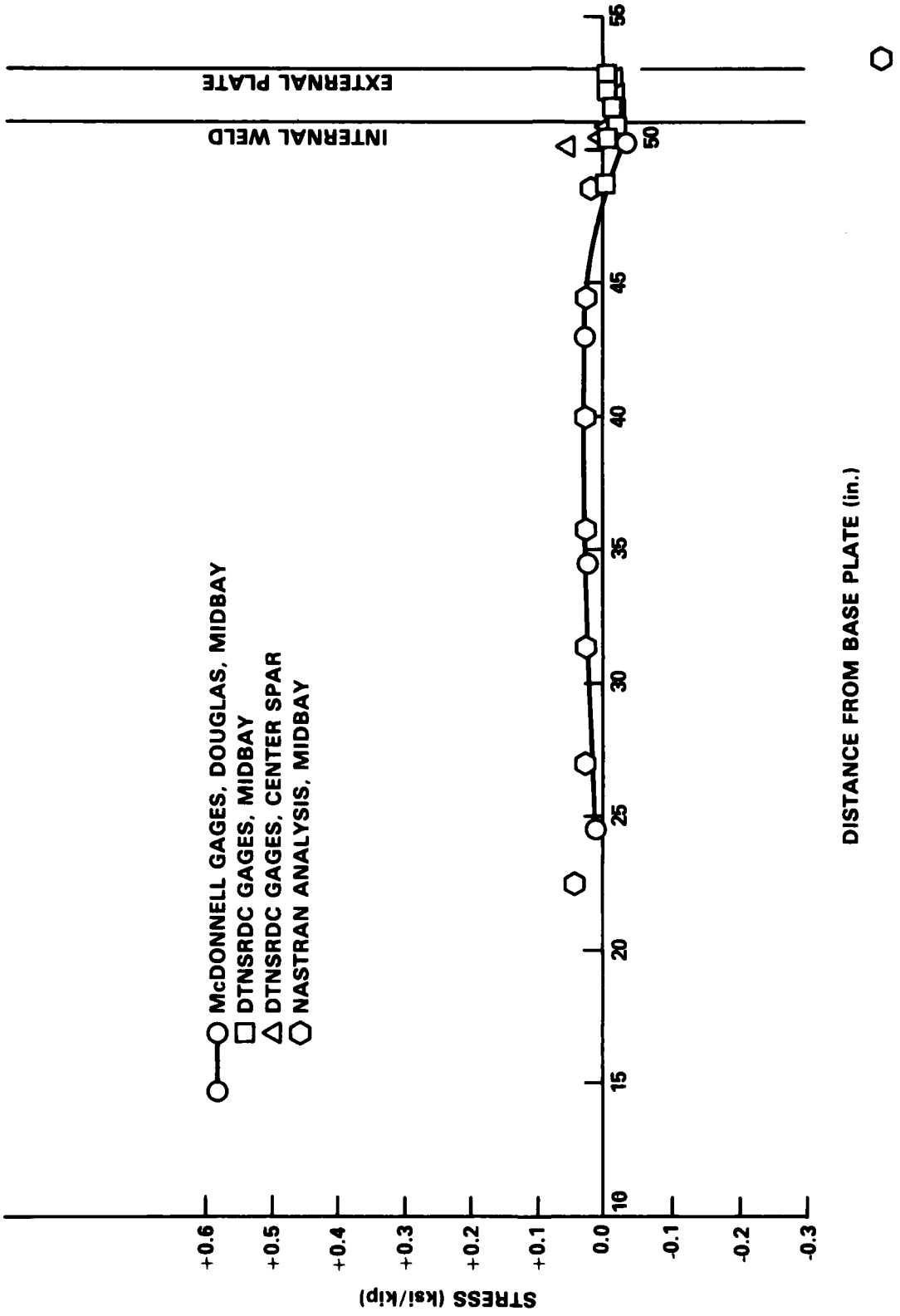

Figure 15 - Transverse Stress versus Longitudinal Distance Along Box Beam

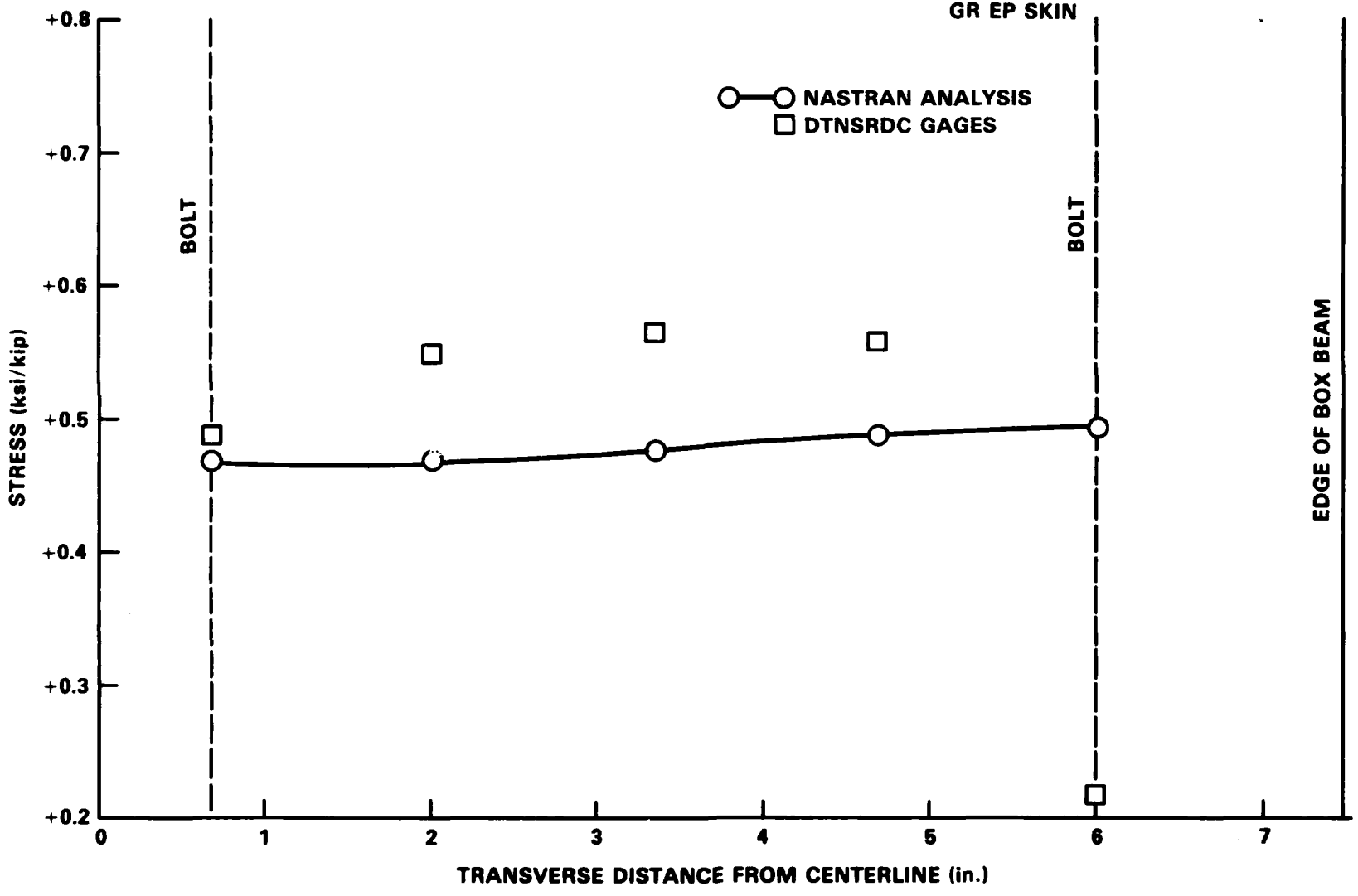

Figure 16 - Longitudinal Stress versus Transverse Distance from Centerline (42.27-in. from Base)

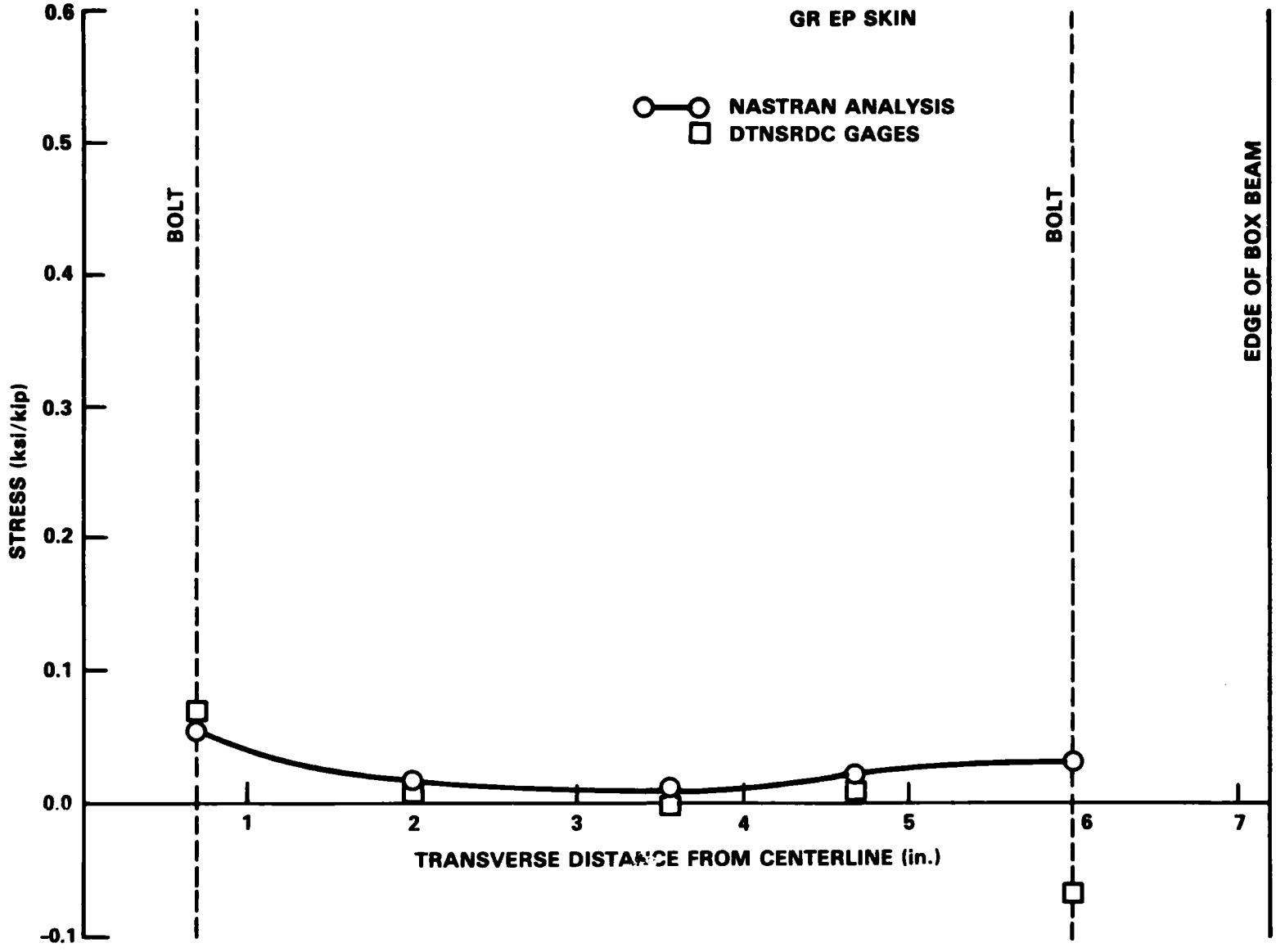

Figure 17 - Transverse Stress versus Transverse Distance from Centerline (42.27-in. from Base)

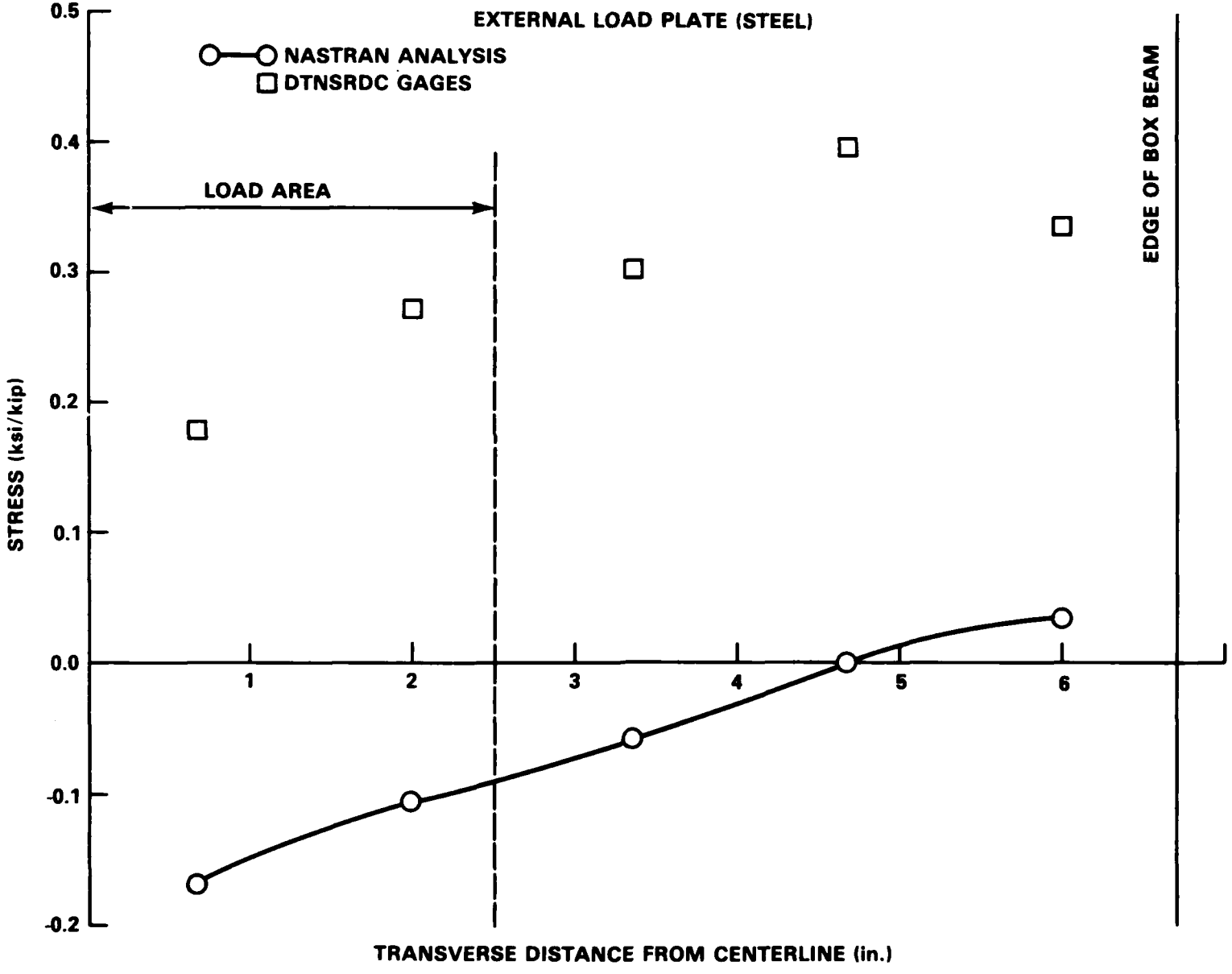

Figure 18 - Longitudinal Stress versus Transverse Distance from Centerline (53.5-in. from Base)

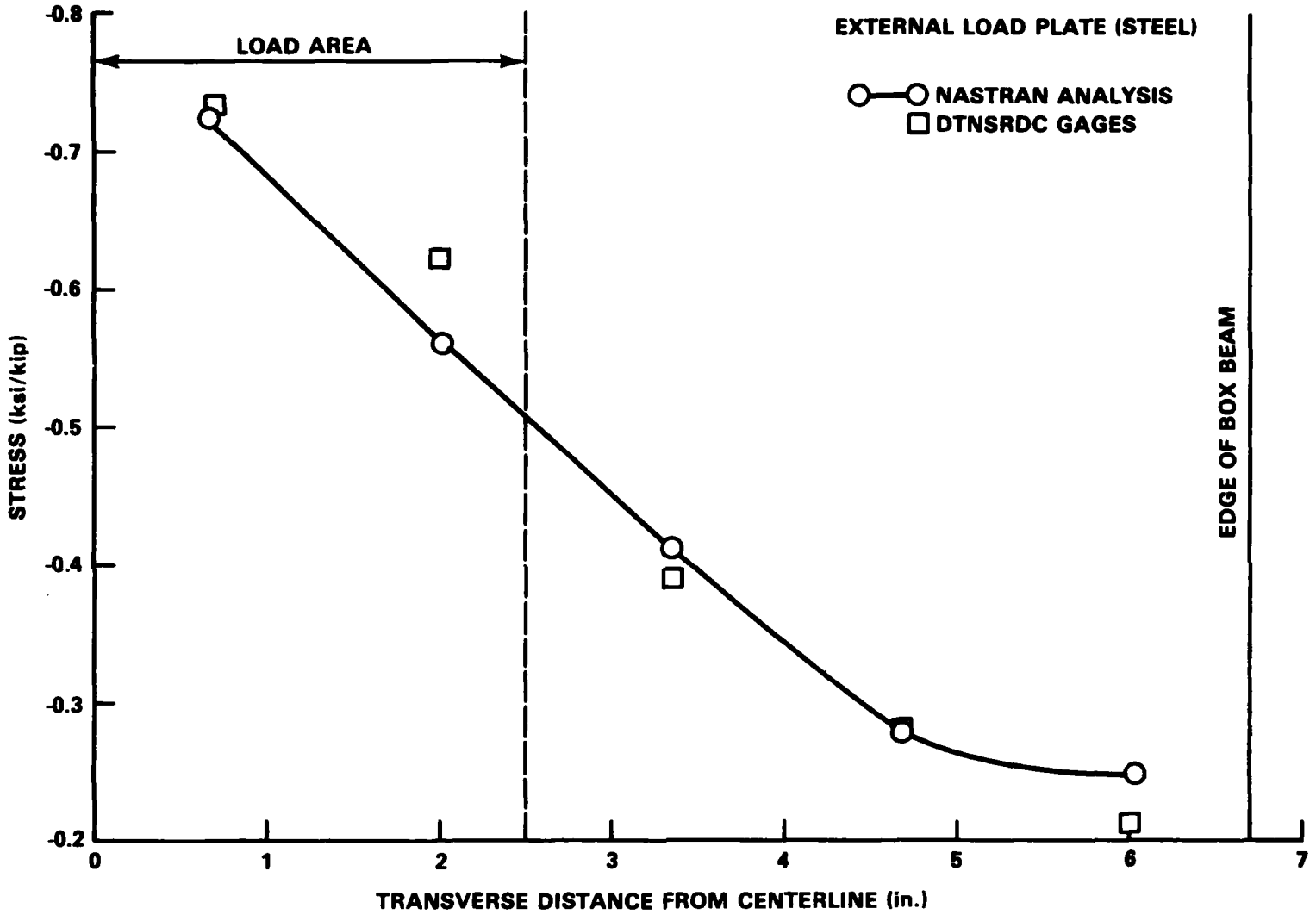

Figure 19 - Transverse Stress versus Transverse Distance from Centerline (53.5-in. from Base)

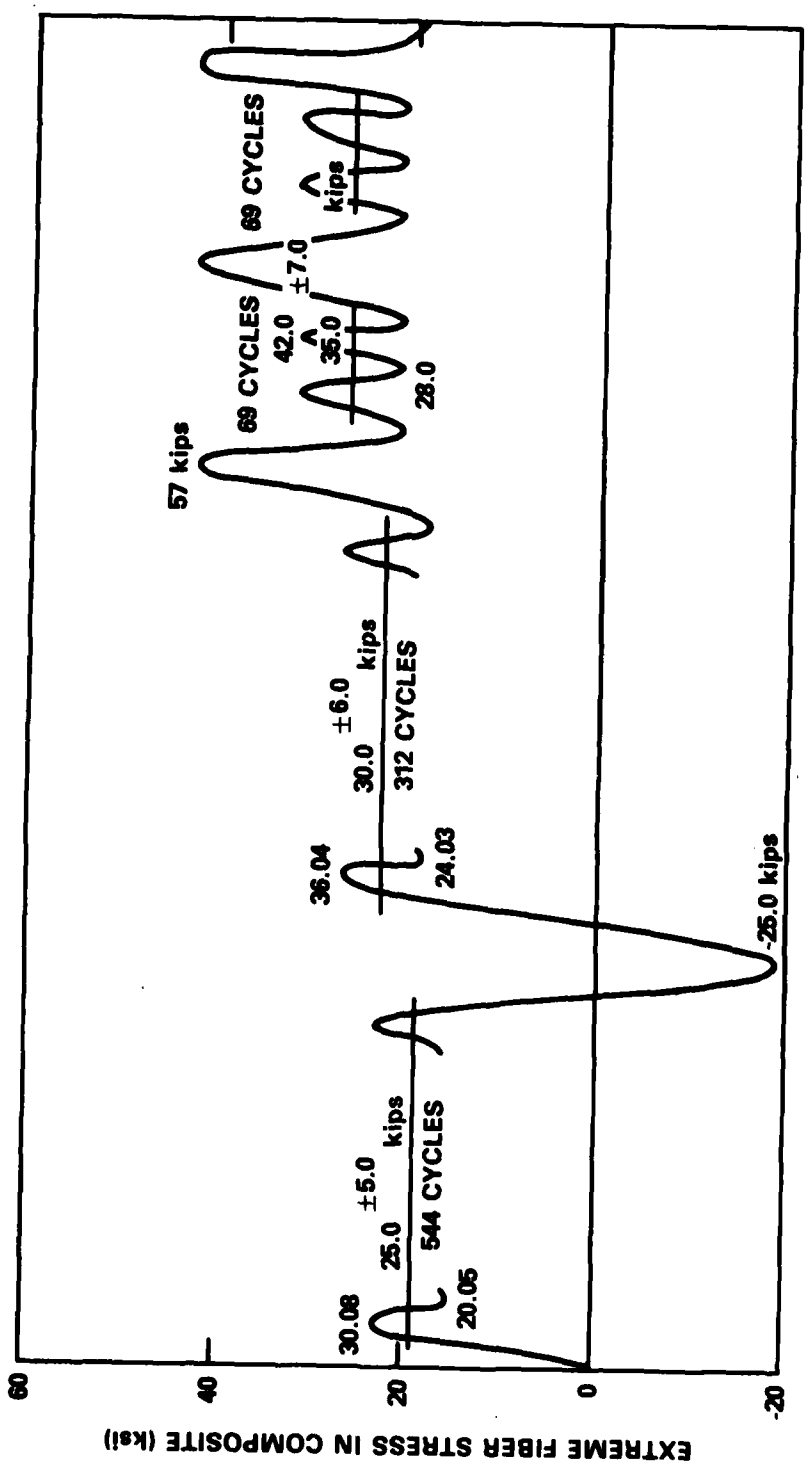

Figure 20 - Fatigue Spectrum for Box Beam 1

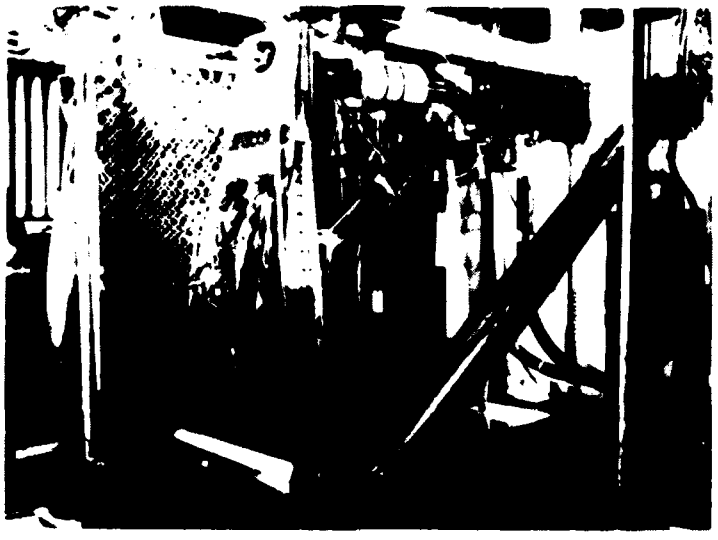

Figure 21a - Overall View

Figure 21b - Closeup Frontal View

Figure 21c - Closeup Rear View

Figure 21 - Box Beam 1 After Catastrophic Failure

at 10,000 cycles and 17,000 cycles due to significant increases in visual delaminations. Deflection measurements were taken during static tests to 57 kips at both intervals to give an approximate indication of the severity of damage incurred as a result of the cyclic tests. The deflections are given in Table 3, and plotted in Figure 22. As can be seen, there were significant changes in overall deflection; an indication that permanent damage may have occurred.

BOX BEAM 2

As indicated in the description of static tests, Box Beam 2 was inspected by manual and SCIMI UT techniques before and after initial static tests to 30 kips. Since the failure of Box Beam 1 could not be analytically explained, nor effective repairs or modifications developed, the cyclic tests of Box Beam 2 did not include the maximum loading condition of 57 kips. Other than this one loading condition, the spectrum was the same as that used for Box Beam 1; hence the maximum loading condition for Box Beam 2 was 42 kips. This load was applied in a single static test, the results of which are given in Tables 7, 8, and 9 for deflections, strains, and stresses, respectively. Since the results did not indicate any damage during this test, the cyclic test was initiated without conducting additional ultrasonic inspection.

The cyclic test was halted after 50,000 and 500,000 cycles for visual inspection and for static tests to measure deflection and strains; see Tables 7 and 8 for results. Also see Figure 23 for plots of deflection versus load. Since there was no gross indication of damage, it was decided to hold the first ultrasonic inspection at 1,000,000. However, after 806,000 cycles, delaminations similar to the initial delamination of Box Beam 1 were discovered during a routine visual inspection. Although the exact time of failure is not positively known, there is good reason to suspect that it occurred after 712,000 cycles. An electrical storm caused a power loss;at which point the test mechanic heard a loud noise which "sounded just like the noise heard when Box Beam 1 failed." He made a quick visual inspection for apparent damage; and since he did not see anything, he did not report it. A manual UT inspection after 806,000 cycles revealed a damage pattern similar to that of Box Beam 1 following its initial failure; however, an inspection of very small flaws found during the original inspection indicated no growth. This factor is another indication that the failure may have been caused by a single overload when the power

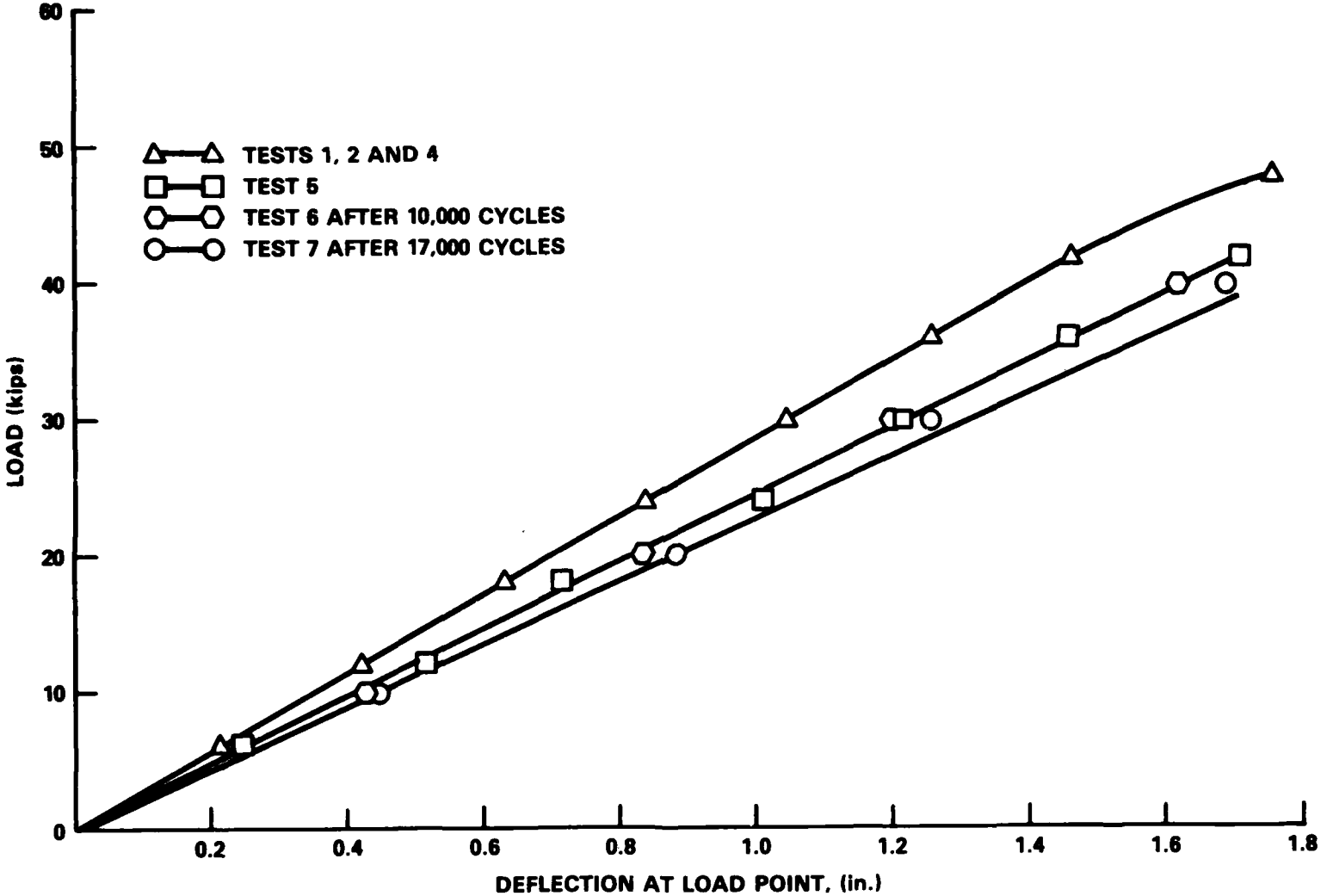

Figure 22 - Changes in Box Beam 1 Deflection Behavior During Cyclic Tests

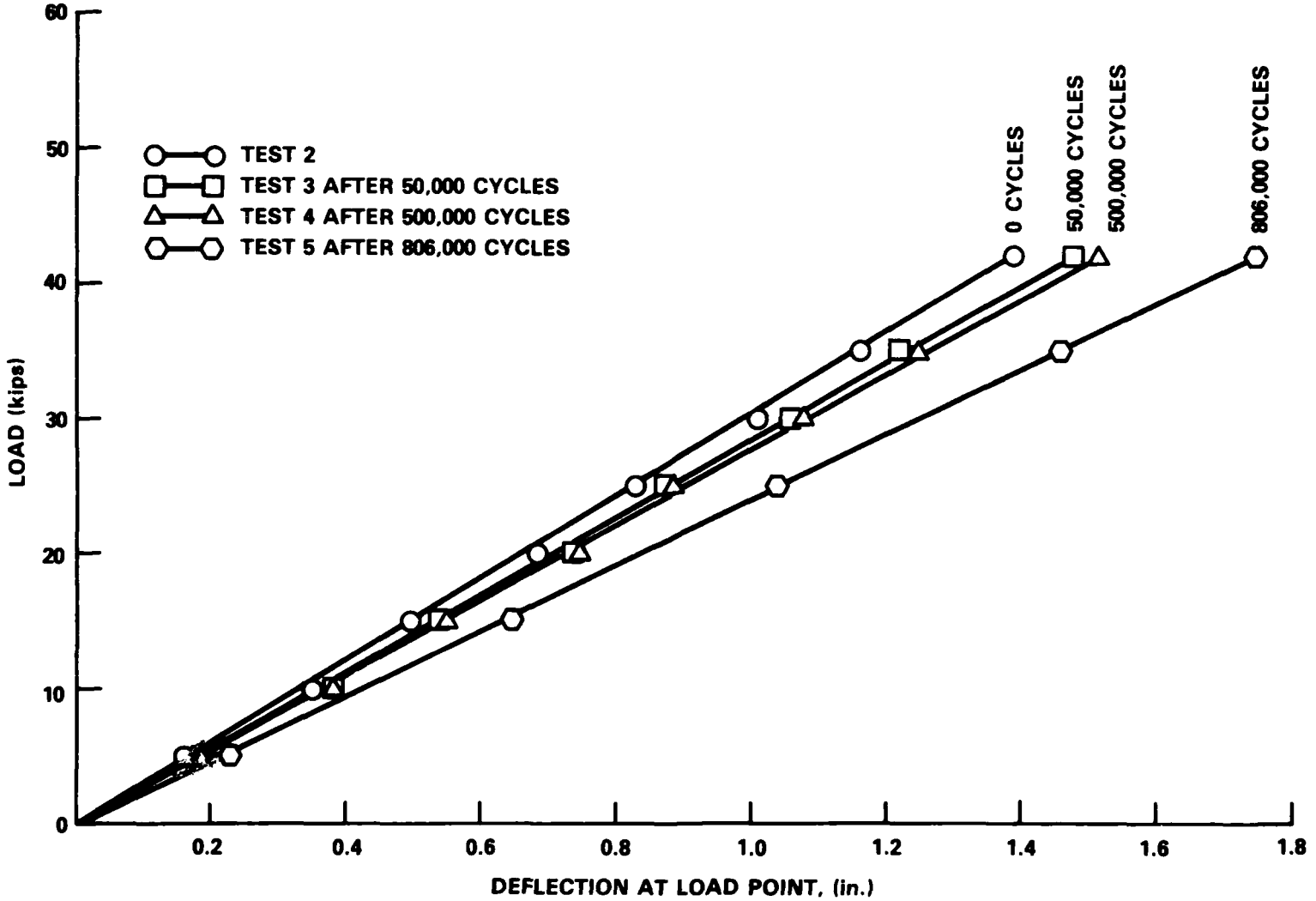

Figure 23 - Changes in Box Beam 2 Deflection Behavior During Cyclic Tests

shut down. A static test in which deflections were measured was conducted; the results are given in Table 7. The cyclic test was resumed, and the box beam failed catastrophically after 920,000 cycles. Figure 24 shows the failed box beam.

EVALUATION OF CYCLIC TEST RESULTS

The results of the cyclic tests of the two box beams were inconclusive. Because Box Beam 1 delaminated prior to attaining the maximum operating load (broach) of 57 kips, leading to a very rapid degradation and ultimate failure, it was impossible to obtain any meaningful evaluation of defect location and growth due to fatigue. Because this load was dropped from the fatigue spectrum for Box Beam 2, and because it unexpectedly failed at an early stage in its intended life, there was no indication of flaw growth associated with Box Beam 2. The best indication of the potential for locating and monitoring the growth of flaws and defects using nondesctructive evaluation was indicated during the static test inspections. The potential for meaningful results in this area is very good, especially with the use of SCIMI or other automated and permanent record collection techniques.

CONCLUSIONS

1. The measured surface stresses in the box beams agreed well with theoretical predictions from the NASTRAN finite element analysis and the conventional design analysis (strength of materials approach).

2. Premature delaminations in the load application area of the box beam most likely occurred as a result of the manner in which the box beam was loaded, i.e., a concentrated load. To eliminate the problem would require: (1) a redesign of the load application area (through more sophisticated analyses and supporting experiments), (2) a large over design of the area based on simple analyses, or (3) modification of box beam geometry (taper).

3. Premature delaminations in the box beam during these tests do not rule out composites as a promising material for hydrofoil applications; it points out a need for a better test technique for composite materials. An improved and more realistic test would be to subject the box beam to a distributed surface loading similar to that seen by an actual foil.

Figure 24a - Overall View

Figure 24b - Closeup Top Rear View

Figure 24c - Closeup Bottom Rear View

Figure 24 - Box Beam 2 After Catastrophic Failure

4. There do not appear to be any reliable experimental techniques for measuring interlaminar shear stresses, nor simple analytical techniques for accurately predicting these stresses as well as the resulting delaminations caused by these stresses.

5. Premature fatigue failure of Box Beam 1 appears to have occurred as a result of overstresses caused by the loss of bending stiffness which took place when the box beam incurred delaminations under static loading.

6. Box Beam 2 delaminated in the load plate region during fatigue testing, apparently as a result of an overload caused by an electrical storm and subsequent power surge.

ACKNOWLEDGEMENTS

The authors would like to express their gratitude to Dr. Milton O. Critchfield, Ms. Maureen R. Tracy, Mr. Douglas E. Paunil, Mr. Jerome P. Sikora, and Mr. Frederick S. Koehler of the Center who provided the analytical efforts and the testing support throughout this project. Mr. Jeffrey E. Beach, Mr. Natale S. Nappi and Dr. Joseph A. Corrado are acknowledged for their technical guidance.

APPENDIX A

LAP JOINT EFFECT

McDonnell Douglas Astronautics Corporation prepared the following calculations for predicting the load required to delaminate the box beam skins. This analysis gives one possible explanation for the observed delaminations.

EFFECTIVE STRENGTH OF BONDED JOINT

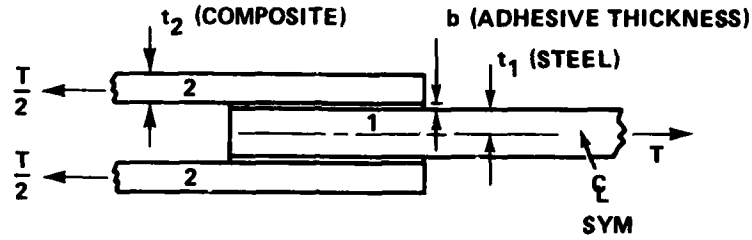

$$\tau_{MAX} = \frac{\beta T}{\alpha} \qquad (1)$$

$$\beta = \frac{G}{bE_2t_2} \qquad (2)$$

$$\alpha = \left\{\frac{G}{b}\left[\frac{1}{E_1t_1} + \frac{1}{E_2t_2}\right]\right\}^{1/2} \qquad (3)$$

TEST RESULTS

T_{ULT} = 18,570 lb (AVERAGE OF THREE TESTS)
t_1 = 0.291 in.
t_2 = 0.237 in.
E_1 = 30×10^6 psi
E_2 = 12.48×10^6 psi
b = 0.0044 in.
G = 60×10^3 psi

FROM EQUATIONS (2) AND (3): $\beta = 4.61$ AND $\alpha = 2.488$
FROM EQUATION (3) THE EFFECTIVE STRENGTH IS: $\tau_e = 17{,}200$ psi

PREDICTED LOAD TO CAUSE DELAMINATION IN BOX BEAM

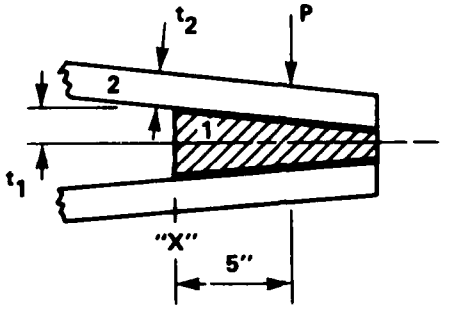

PROPERTIES AT TRANSITION POINT "X"

t_1 = 0.59 in.

t_2 = 0.50 in.

$E_1 = 30 \times 10^6$ psi

$E_2 = 12.48 \times 10^6$ psi

b = 0.0044 in (ASSUME SAME AS JOINT)

$G = 60 \times 10^3$ psi (ASSUME SAME AS JOINT)

FROM EQUATIONS (2) AND (3): $\beta = 2.19$ AND $\alpha = 1.717$

FROM EQUATION (1): T = (17,200)(1.717)/2.19 = 13480 lb

CORRESPONDING STRESS $\sigma_0 = T/t_2 = 26{,}960$ psi

BENDING STRESS AT "X" ON INSIDE SURFACE (EQUIVALENT I = 5.28)

$$\sigma_B = \frac{5Pt_1}{I} = 0.559\ P$$

EQUATING σ_B TO σ_0 AND SOLVING FOR P

P = 48,230 lb

APPENDIX B

SAP 4 ANALYSIS

In order to investigate the interlaminar stresses in the box beam skins, a three-dimensional finite element analysis, SAP 4, was carried out at Virginia Tech.* It was possible to model the skins as being composed of three layers: the two outer layers of four plies of T-300 at 0 deg each and the internal core layer of T-300 at 0 deg and GY 70 at $\pm$ 45 deg. This was significant since the delaminations observed occurred between these layers. The elastic properties used in this analysis are found in two ways: the properties with respect to the x and y direction were generated from lamination theory; and the z direction properties were estimated.

There were four different models run to study the effect of the order of Gaussian integration used and the use of shear panels versus three-dimensional elements in the spar-web regions. Each of these analytical cases produced different results, and all differ from NASTRAN and from experiment.

Although Va. Tech could not give quantitative answers, some qualitative conclusions were made. They did find high through-the-thickness normal stresses in the load block region as well as high through-the-thickness shear stresses and transverse normal stresses. There were abrupt changes found between the layers in the skins. The analysis would predict splitting on the tension side and buckling on the compression side from this last observation.

The high interlaminar stresses were believed to be due to rigid constraints attributed to the steel load blocks and solid interior. These stresses were believed to be complicated by a large mismatch in transverse material properties between the two materials in the skins. It was suggested that the restraints be removed and the load be distributed. A SAP 4 run was made of this case and it was found to be effective in reducing the normal stress but not the shear stresses.

---

*Wong, D.A., "Finite Element Analysis of a Composite Box Beam," M.S. Thesis, Virginia Polytechnic Institute and State University, Blacksburg, Virginia (May 1980).

APPENDIX C

EFFECT OF VARIATION OF LOAD APPLICATION

Using basic beam bending equations and cross-sectional properties, an attempt was made to calculate the effect of modifying the load application (load and location). It was thought to be possible to obtain less shear stress in the load region while maintaining the same bending stress by extending the point of load application and varying the load. Table C.1 and Figure C.1 demonstrate the current situation (A) and the proposed one (B). It is seen that varying the load application causes an undesirable disturbance in the bending stress and, therefore, was discarded.

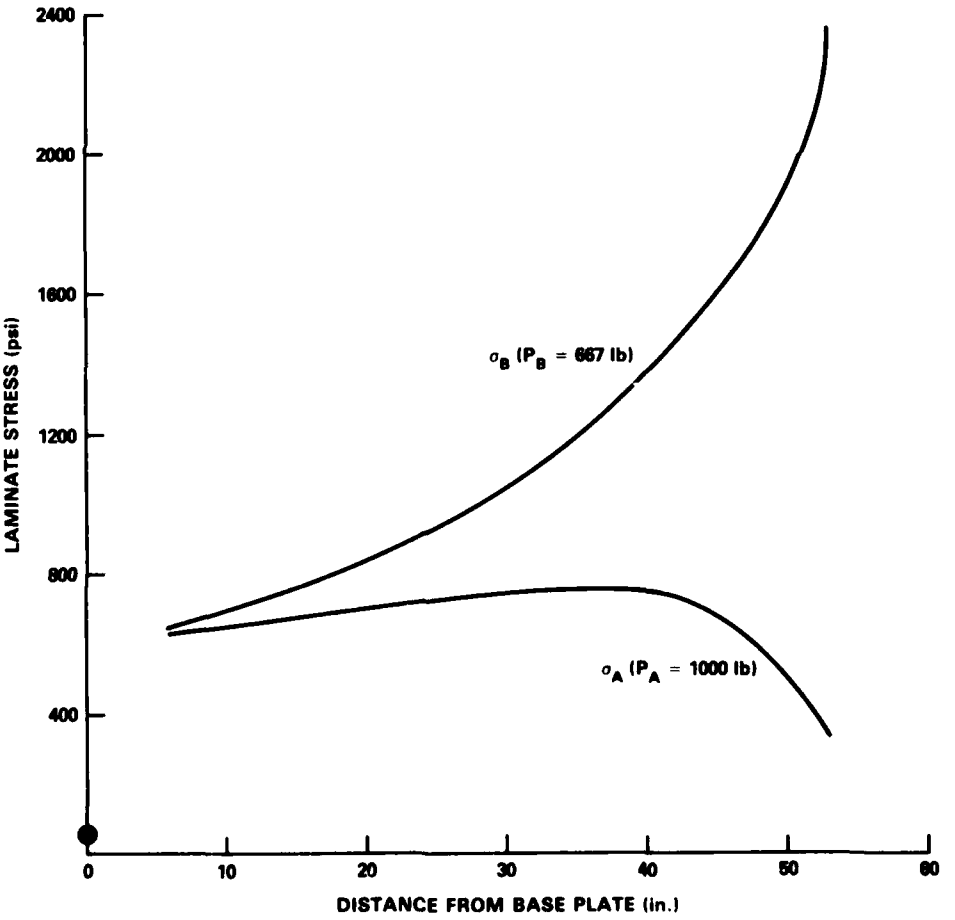

Figure C.1 - Comparison of Box Beam Stresses for Change in Load Application

TABLE C.1 - STRESS CALCULATIONS FOR CHANGE IN LOAD APPLICATION

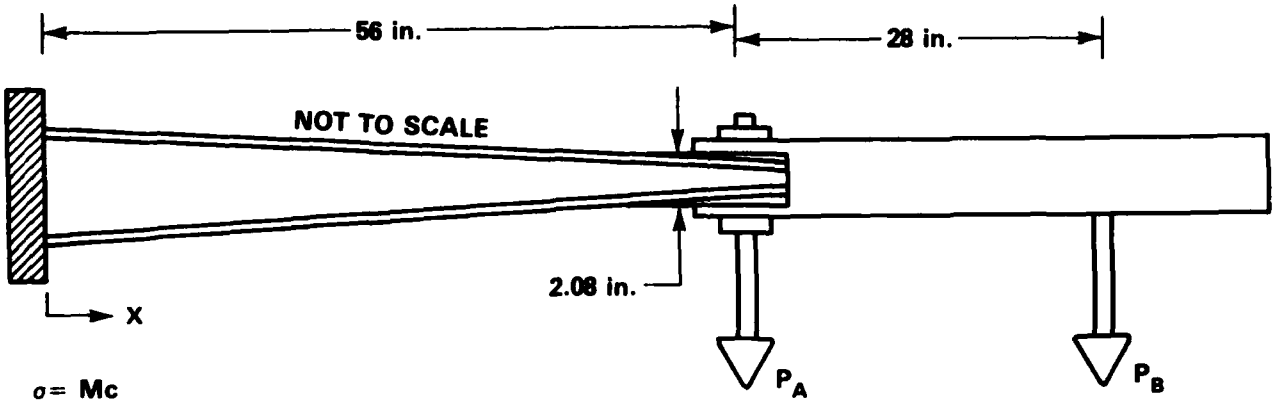

$$\sigma = \frac{Mc}{I}$$

$$\tau = \frac{VQ}{It}$$

P_A = 1000 lb

P_B = 667 lb

X	I	C	C/I (X1000)	σ_A	σ_B
0	302.0	3.25	1.08	60.5	60.5
6	238.4	3.00	12.58	629.	645.
9	209.0	2.88	13.78	648.	689.
13	174.9	2.71	15.56	669.	737.
18	138.0	2.50	18.12	689.	798.
23	105.0	2.29	21.81	719.	887.
30	69.2	2.00	28.9	751.	1041.
33	56.9	1.88	33.0	759.	1123.
38	39.5	1.67	42.3	761.	1298.
43	26.4	1.46	55.3	719.	1512.
48	17.0	1.25	73.5	588.	1765.
53	9.1	1.04	114.3	343.	2363.

REFERENCES

1. Greszczuk, L.B. and Hawley, A.V.,"Advanced Composites and Their Application to Patrol Craft Hydrofoils," McDonnell Douglas Astronautics Co. Final Report on work performed for the Naval Sea Systems Command under Contract N00024-72-C-5536 (Apr 1973).

2. Grumman Aerospace Corporation, "Investigation of Composite Material for Use in Light Weight Hydrofoil Structures," Final Report on work performed for the Naval Sea Systems Command under Contract N00024-74-C-5048 (30 Sept 1974).

3. Greszczuk, L.B. and Couch, W.P., "Design, Fabrication and Nondestructive Evaluation of an Advanced Composite Foil Test Component (Tapered Box Beam)," American Society for Testing and Materials, Special Technical Publication (STP 674), pp. 84-100 (1979).

4. Greszczuk, L.B. and Ashizawa, M., "Advanced Composite Foil Test Component (Tapered Box Beam)," McDonnell Douglas Astronautics Company, Final Report MDC-G7596, (May 1977).

5. Chaskelis, H.H., "Ultrasonic Inspection of a Graphite/Epoxy Structural Member Using a Thickness-Imaging Device," Naval Research Laboratory Memorandum Report 4473 (20 Mar 1981).

6. Jones, R.M., "Mechanics of Composite Materials," McGraw-Hill Book Company (1975).

7. Critchfield, M.O., "Structural Analysis Methods and Elastic Property Determination for Laminated Composites," DTNSRDC Report 81/018 (Aug 1981).

INITIAL DISTRIBUTION

Copies

11	NRL
	1 6383 (Wolock)
	10 5834 (Chaskelis)
6	NAVSEA
	1 SEA 05E3 (White)
	1 SEA 05R (Gagorik)
	1 SEA 05R (Vanderveldt)
	1 SEA 55Y (Aronne)
	1 SEA 55Y1
	1 SEA 55Y2
3	The Boeing Company
	1 Sam Oken
	1 Howard Johnson
	1 John Hoggatt
10	McDonnell Douglas Astronautics Company
	10 Longin Greszczuk
12	DTIC

CENTER DISTRIBUTION

Copies	Code	Name
1	11	
1	115	
2	1152	
1	17	
1	1702	
1	1706	(m)
1	1720.6	
1	1730	
1	1730.1	
1	1730.2	
1	1730.4	
1	1730.5	
1	1730.6	
10	1730.6	(Couch)
1	177	
1	1770.4	(m)
1	2823	(Macander)
10	5211.1	Reports Distribution
1	522.1	Unclassified Lib (C)
1	522.2	Unclassified Lib (A)

END

FILMED

1-83

DTIC